Diploma Thesis

The Chick Chorioallantoic Membrane as an In-Vivo Xenograft for Human Skin in Regenerative Medicine

A model for studying ischemic wounds and the regeneration process of CAM integrated skin grafts

submitted by

Cand. med. Georg Kornhäusel

in order to obtain the academic degree

Doctor medicinae universae

(Dr. med. univ.)

at the

Medical University of Graz

Department of Surgery

Division of Plastic, Aesthetic and Reconstructive Surgery

under supervision of

Ass. Dr. Christian Smolle

Univ. Prof. Dr. med. Lars-Peter Kamolz, MSc

Graz, 25th. of September 2019

Declaration in lieu of oath

I, herewith, declare that I have written the following diploma thesis fully on my own and without any assistance from third parties. Furthermore, I confirm that no sources have been used in the preparation of this thesis other than those indicated in the thesis itself. Any thoughts directly or indirectly taken from somebody else's sources are made discernible as such.

Graz, 25th. of September 2019 *Georg Kornhäusel eh*

Preface

As a rather young discipline of life sciences, regenerative medicine concentrates on the renewal of cells, tissues as well as organs in their whole complexity and function and therefore especially on the wound healing process with consequences in human medicine e.g. acute and chronic wound treatments.

According to "Epidemiology of chronic wounds in Germany: Analysis of statutory health insurance data" by Heyer et.al. (1) in 2012 1.04% of insured patients in Germany had a wound diagnosis, including 0.70% with chronic wounds, prevalence and incidence increasing over 3 years (1). Wound healing enables tissues not to lose their functions as well as it ensures the integrity of the human body. The understanding of all the components of this process and their interactions not only leads to an improvement of health, quality of life and medical care of patients, but also helps in the development of in-vitro tissues and organs in tissue engineering.

Although, many achievements in regenerative medicine have already been recorded, there is quite a lot more to understand. Only by focussing on the understanding of wound healing - the basis of all regenerative processes in humans – new therapies, treatments and much more can result.

With the development of an in-vivo chick chorioallantoic membrane (CAM) model for ischemic wounds, we intend to study the impact of ischemia on the wound healing process. Since the developing chicken embryo lacks B- and T-cell mediated immune response (2), this model is most suitable as an in-vivo xenograft model and therefore for studying the role of ischemia. In addition to this, it is shown, that the CAM assay is superior to the classic in-vitro models and therefore an alternative to animal testing.

Based on this diploma thesis, new models in research concerning chronic wounds, especially ischemic ones, will be implemented. Furthermore it will allow to study the impact of interventions and pharmacological substances on ischemia and the wound healing process in order to generate new therapies.

Acknowledgments

First of all I want to thank Ass. Dr. Christian Smolle. With advice and assistance he supported me throughout the whole research project – from the theoretical to the practical implementation.

Furthermore, I want to thank Univ. Prof. Dr. Lars-Peter Kamolz, MSc for the opportunity to take my first steps in Regenerative Medicine. Due to his professional expertise on the implementation of research projects a rather quickly realisation of our ideas was possible.

In addition to this, I am deeply grateful for the help of Univ.-Ass.in Mag.a Dr.in Nassim Ghaffari Tabrizi-Wizsy. As an expert on the development and application of the CAM in medical research, she paved the way for high level laboratory work. Nearly available around the clock, Univ.-Ass.in Mag.a Dr.in Nassim Ghaffari Tabrizi-Wizsy supported me with an unbreakable enthusiasm, with useful ideas, suggestions and help.

Research questions of a certain complexity required the knowledge of further scientists. For this reason I want to thank Univ. Prof. Mag. pharm. Dr. rer. nat. Wolfgang Graier, head of the Gottfried Schatz Research Center, Divison of Molecular Biology and Biochemistry, who helped us in finding the correct illumination system for our experiments, as well as Tony Schmidt, MSc, from the Divison of Biophysics for the help in pulling micropipettes for our injections.

Finally, my thanks also go to Kathrin Kreuzer and Waltraud Huber for their help in laboratory work, the Department of Plastic, Aesthetic and Reconstructive Surgery Graz, COREMED, Joanneum Research, Gottfried Schatz Research Center and the Otto Loewi Research Center for Vascular Biology, Immunology and Inflammation for the supply with laboratories, materials and research funds.

Last of all, I am really grateful for my family, who made it possible for me, not only to study human medicine, but also to live in Graz. Although it was not always easy for them, they fully supported me with all the possibilities they could provide.

Abstract

Introduction

Wound healing is a complex process consisting of several phases and requiring an ideal interaction between cellular and biochemical factors. An essential step of this regenerative process is adequate supply of the wound area with oxygen and nutrients by neovascularisation. This enables cell proliferation and biochemical synthesis procedures to renew tissue. Ischemia or simply inadequate blood supply of tissues can lead to the formation of chronic wounds. Approximately 1 percent of the population in Germany suffer from chronic wounds, incidence and prevalence increasing (1). Therefore, a number of studies are needed to develop models, which can be used for studying the complexity of the regeneration process of human skin (3). This understanding will lead to new products and therapies for patients. With this diploma thesis we aim to establish methods to develop a new model for studying ischemic wounds and the regeneration process of human skin based on chick chorioallantoic membrane integrated split skin grafts.

Material and Methods

Chick chorioallantoic membrane assays were cultured following an established ex-ovo method from Deryugina et.al. On day 7 split skin grafts were transferred onto the CAM. After 3 days full integration of the xenografts into the CAM was detected. Using a special pulled micropipette 3 µL of a 50mg/mL solution of Rose bengal was applied intravenously and by means of a 120W cold light lamp and a 525/50nm filter the photothrombosis was induced after the selection of an appropriate CAM area.

Results

The results obtained in the diploma thesis indicate that grafting of human skin on the chick chorioallantoic membrane, the injection of Rose bengal in CAM blood vessels, the haemostasis of bleeding and the induction of photothrombosis are successfully implemented. A typical pattern of vessel changes could be observed. After 8min of illumination an obvious reduction of vessel density and a visible decrease of the vessel lumen could be seen.

Discussion

The follow-up of ischemic wounds was not yet possible, since the chicken embryos only survived hours after treatment. We assume that this may be because of a certain dosage dependent toxicity of Rose bengal in the developing chicken embryo or the blood loss – some millilitres - appearing after the injection process.

Zusammenfassung

Einleitung

Wundheilung – ein komplexer Prozess aus mehreren Phasen, der ein ideales Zusammenspiel aus zellulären und biochemischen Faktoren benötigt. Der entscheidende Schritt dieses regenerativen Prozesses besteht dabei in einer adäquaten Versorgung des Wundareals mit Sauerstoff und Nährstoffen durch Neovaskularisation. Nur dadurch werden Zellproliferation und biochemische Syntheseprozesse ermöglicht, um Gewebe zu erneuern. Eine unzureichende Blutversorgung, auch Ischämie bezeichnet, führt zur Entstehung chronischer Wunden. Etwa 1 Prozent der deutschen Bevölkerung leidet an chronischen Wunden, Prävalenz und Inzidenz steigend (1). Aus diesem Grund bedarf es eine Reihe von Experimenten zur Entwicklung neuer Modelle, um den regenerativen Prozess der menschlicher Wundheilung erforschen zu können. Dieses Wissen bildet die Grundlage für neue Produkte und Therapien. Ziel der Diplomarbeit ist es, neue Methoden für Modelle der Wundheilungsforschung insbesondere für ischämische Wunden zu etablieren.

Material und Methoden

Chick Chorioallantoic Membrane (CAM) Assays wurden nach einer etablierten ex-ovo Methode nach Deryugina et.al. kultiviert. Am 7. embryonalen Entwicklungstag wurden Spalthauttransplantate auf den CAM Assay übertragen. Integration und Versorgung durch CAM Gefäße zeigte sich nach 3 Tagen. Mittels einer Mikropipette wurden nun 3 µL einer 50mg/mL Rose bengal Lösung intravenös appliziert und mit Hilfe einer 120W 525/50nm starken Kaltlichtquelle, um die Photothrombose im gewünschten Areal zu induzieren.

Resultate

Die Ergebnisse der Diplomarbeit zeigen, dass das Kultivieren menschlicher Spalthaut auf CAM Assays, die Injektion von Rose bengal in CAM Gefäße, die Hämostase blutender Gefäße und die Induktion der Photothrombose möglich sind. Ein typisches Muster an Gefäßveränderungen konnte beobachtet werden. Nach 8min Bestrahlung zeigte sich eine deutliche Reduktion des Gefäßdichte, wie auch des Gefäßlumens im ausgewählten Areal.

Dikussion

Ein Follow-up der ischämischen Wunden war im Rahmen der Diplomarbeit noch nicht möglich, da die Hühnerembryonen das Prozedere nur einige Stunden lang überlebten. Dies könnte an einer dosisabhängigen Toxizität von Rose bengal bei sich entwickelnden Hühnerembryonen oder aber auch am Blutverlust - einige Milliliter - nach erfolgter Injektion liegen.

Content

Glossary and Abbreviations

ATP	adenosine triphosphate
bFGF	basic fibroblast growth factor
CAM	chick chorioallantoic membrane
ECM	extra cellular matrix
e.g.	example given
EGF	epidermal growth factor
EtOH	ethanol
FGF-2	fibroblast growth factor 2
i.e.	id est
IGF-1	insulin-like growth factor 1
IL-1α	interleukin 1α
IL-1β	interleukin 1β
IL-6	interleukin 6
IL-8	interleukin 8
MMP	matrix metalloproteinases
PBS	phosphate buffered saline
PDGF	platelet derived growth factor
ROS	radical oxygen species
TGF-α	transforming growth factor alpha
TGF-β	transforming growth factor beta
TGF-α	transforming growth factor alpha
TNF	tumor necrosis factor
TNF-α	tumor necrosis factor alpha
VEGF	vascular endothelial growth factor

Table of Figures

List of Tables

1 Introduction

1.1 Histology of Epithelial Tissue

Epithelial tissues are complexes consisting of polarized cells, that are closely connected to each other by cellular contacts and fixed on a basal membrane. Due to these epithelial tissues are boundary forming units that separate the extracellular space into compartments. Depending on their function 2 major types of epithelial tissue are differentiated: Surface epithelium and glandular epithelium. All epithelial tissues can develop from the ecto-, meso-, and entoderm (4).

1.1.1 Overview

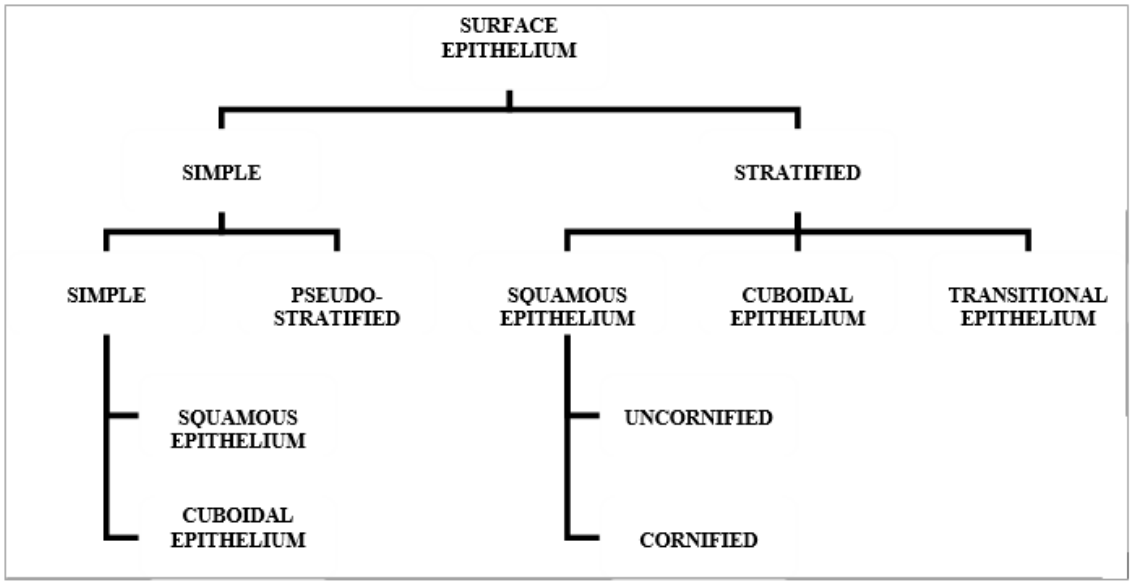

Figure 1: Overview on types of surface epithelia
from (4)

For the classification of surface epithelium, there are two main criteria: the number of cell layers and the shape of the cells e.g. cuboidal or squamous (4).

1.1.2 Stratified Epithelium

Characterised by more than 10 layers of cells, stratified epithelium can be found wherever high mechanical stress exists. The cells are fixed to the basal membrane with hemidesmosomes and have a dense network of cytokeratin filaments, that are linked in between the cells with desmosomes (4).

1.1.3 Stratified Squamous Cornified Epithelium

Stratified squamous cornified epithelium is built by so called keratinocytes that form special layers (4) (5): Stratum basale, Stratum spinosum, Stratum granulosum and Stratum corneum.

The process of cornification starts in the Stratum granulosum, where keratohyalin granules can be found. These cytoplasmatic granules are excessively stainable and consist of cytokeratin filaments which are tightly connected with proteins. Completely cornified cells build the Stratum corneum. Cornified cells are characterised by a non-nucleated devitalised state and a dense network of crosslinked cytokeratin filaments which fill the whole cell (4).
One of the most important functions of stratified epithelium is to be a diffusion barrier with polar lipids occluding the intercellular space. In addition a continuous network of tight junctions exists (4).
Since the lifetime of cells is limited to approximately 30 days in epidermis, permanent renewal is necessary for the integrity of surface epithelium. Therefore the cycle consisting of cell proliferation, cell differentiation and apoptosis has to be strictly regulated (4).

1.1.4 Human Skin

From a histological point of view the human skin can be divided into two sections: the cutis and the subcutis. Whereas cutis is the umbrella term for epidermis and dermis, the subcutis only describes connective and fatty tissue below the cutis.
Epidermis, dermis and subcutis form the so-called cutaneous covering or Integumentum commune. Most of the human body is covered with hairy skin, only the palms and soles are covered with glabrous skin (4) (5).

1.1.4.1 Epidermis

The epidermis is about 75-150µm thick in areas of hairy skin, up to 600µm on palms and soles (6). As a stratified cornified squamous epithelium the epidermis protects the human body (4) and builds a landscape of fractal geometric shapes on the surface (6).
The main cell that can be detected in epidermis is the keratinocyte. Furthermore, melanocytes, Langerhans' cells and Merkel cells are located in this skin layer.
Dividing the epidermis into 4 layers, vital cells build the lower three. Dead keratinocytes can only be found in the uppermost one (4).
Throughout the differentiation process, keratinocytes migrate from the Stratum basale up to the Stratum corneum, undergo apoptosis and become completely cornified (4).

1.1.4.1.1 Layers of Epidermis:

- Stratum basale: adjacent to the basal membrane the purpose of this one layer of columnar cells is cell proliferation. For this reason, mitosis can only be found here. Stem cells, progenitor cells and melanocytes are located in this layer (4).

- Stratum spinosum: it consists of several layers of polygonal keratinocytes and Langerhans' cells (4).
- Stratum granulosum: about three layers of squamous cells with keratohylin granules can be detected by the use of light microscope (4).
- Stratum lucidum: with cells at an intermediate stage between keratinocytes and corneocyte, the Stratum lucidum can only be seen in glabrous skin (4).
- Stratum corneum: here, non-nucleated corneocytes that are fully differentiated, can be seen. On the surface a permanent desquamation takes place (4).

1.1.4.2 Dermis

Stratum papillare and the Stratum reticulare are the two layers that build the dermis (4):

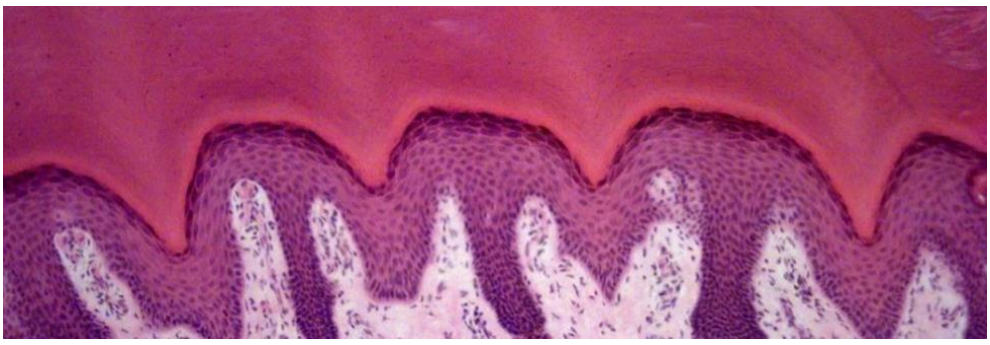

Figure 2: Layers of epidermis
from (7)

- Stratum papillare: it consists of the overall of papillae as well as loose connective tissue with collagen fibers, especially Type III and I, elastic fibers and lots of cells. Every papilla has its own capillary loop and nerve endings.
- Stratum reticulare: composed of dense connective tissue with collagen fibers, especially Type I, and elastic fibers, this layer is responsible for mechanical resistance of the skin.

1.1.4.3 Subcutis

The subcutis or hypodermis is the lowest layer of human skin. It consists mainly of fatty tissue with the epifascial nerves and vessels (4). It is rich in proteoglycan and glycosaminoglycans to attract fluid. Fibroblasts, adipose cells and macrophages can mostly be found in the hypodermis (6).

1.2 Wound Healing and Regeneration

To maintain the integrity of the human body, the skin has to be able to heal - in other words to regenerate. Therefore the wound healing process, consisting of different stages, is a complex mechanism of soluble mediators, blood cells, extracellular matrix and parenchymal cells (8). Imbalance of stimulating and inhibiting factors cause failure of healing, with e.g. ischemia as a major cause of wound repair dysregulation (9).

Depending on the result of the wound healing process, we distinguish between "regeneration" and "skin repair". Regeneration is the specific substitution of the tissue, whilst skin repair describes an unspecific form of healing in which the wound heals by fibrosis and scar formation (10) (11).

Although until now, wound healing is not completely understood, the process can be divided into three phases: inflammation, tissue formation and tissue remodeling (12). These three phases do not take place one after another, but they overlap in time (8).

In "Wound Repair and Regeneration" by J.M. Reinke and H. Sorg from the Department of Plastic, Hand and Reconstructive Surgery, Hannover Medical School in Germany, physiological responses have been described – more precisely the vascular response and the cellular one. These physiological responses are responsible for homeostasis, the formation of a provisional wound matrix followed by an inflammation process, cell proliferation, repair and remodeling (10).

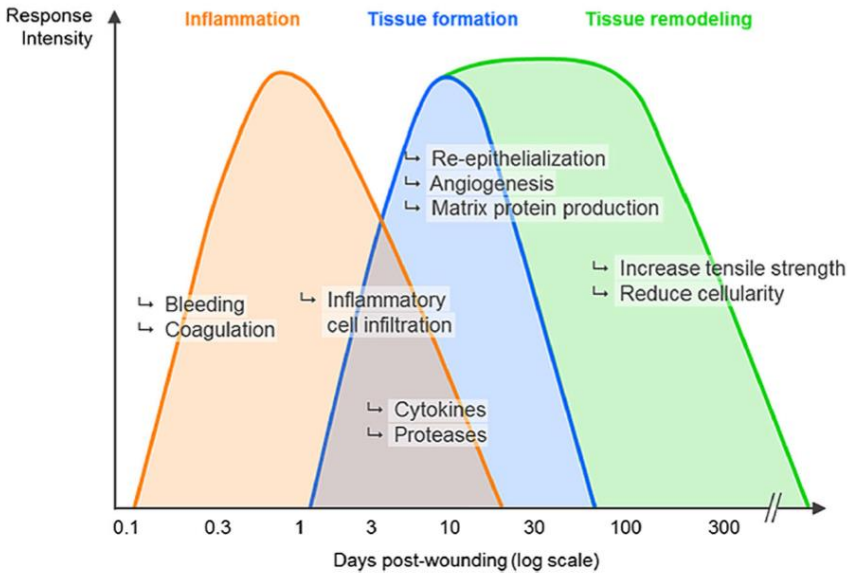

Figure 3: Phases of skin repair
from (13)

1.2.1 Vascular Response

After skin trauma, the epidermal layer, blood and lymphatic vessels are injured. The extrinsic clotting system gets activated by clotting factors from the injured skin, whilst thrombocytes react to the exposed collagen, the intrinsic system, and form aggregates. These aggregates consist of fibrin, fibronectin, vitronectin and thrombospondins – the ideal medium for the migration of cells. For the next 5 to 10min a vasoconstriction of the surrounding vessels helps minimizing the blood loss, too, and leads to a reduction of tissue perfusion, generating increased glycolysis and pH-changes. After vasoconstriction, vasodilatation enables thrombocytes to invade the provisional wound. Not only that thrombocytes build the blood clot, but they also release chemotactic factors to attract different leukocytes. Cytokines and growth factors of both thrombocytes and leukocytes are necessary to initiate the inflammatory reaction (IL-1α, IL-1β, IL-6, TNF-α), to stimulate collagen synthesis (FGF-2, IGF-1, TGF-β), to activate the transformation of fibroblasts to myofibroblasts (TGF-β) and to support the reepithelialisation process (EGF, FGF-2, IGF-1, TGF-α) (10).

1.2.2 Inflammation

Initiated by cytokines and growth factors of thrombocytes and leukocytes the inflammatory phase is crucial for supplying growth factors and cytokine signals, that are needed for cell and tissue movements during the wound healing process. Two phases can be described: in the early phase neutrophil granulocytes appear, in the late phase the appearance and transformation of monocytes can be detected (10).

Damage-associated molecular patterns or pathogen-specific molecular patterns, recognised by toll-like receptors, help initiating and pushing forward the inflammation process. Leukocytes use the gradient of chemokines to migrate to the site of injury (14).

Recruited neutrophils are present for 2-5 days unless there is infection. The neutrophils phagocytose bacteria and secrete proteases to kill microorganisms. They also secrete chemo-attractants for other cells. TNF-α, IL-1β and IL-6 intensify inflammation and stimulate VEGF and IL-8 for the repair process (10).

Macrophages enter the wound area after 3 days (10). Skin resident macrophages and differentiated monocytes are activated by pathogen-specific patterns and damage-associated molecular patterns. At the very beginning of wound repair they differentiate into the M1 subset (14). Like neutrophils, M1 macrophages perform phagocytosis and secrete growth factors (TGF-β, TGF-α, basic FGF, PDGF, VEGF), chemokines and cytokines for the maintenance of wound healing and for the activation of cell proliferation (10). Later they transform into the M2 subset of macrophages. They synthesise anti-inflammatory mediators,

produce the ECM, initiate the proliferation of fibroblasts and the angiogenetic process. M2 macrophages also phagocytose neutrophils, bacteria and cell debris. A failure in the M1-M2 transition leads to nonhealing or chronic wounds (14).

1.2.3 Tissue Formation

Approximately 3-10 days after injury, the proliferation phase starts. The main purpose is to cover the wound surface, to form granulation tissue and to restore the vascular system (10).

1.2.3.1 Re-epithelialization

At the very beginning local fibroblasts immigrate along the fibrin network, whilst also reepithelialisation from the wound edges and neovascularisation/angiogenesis are present. The new matrix of connective tissue is built by the synthesis of collagen, fibronectin and other basic substances, slowly increasing over time, whilst the proliferation of fibroblasts declines (10). Re-epithelialization starts some hours after injury by conversion of cobblestone-shaped stationary keratinocytes into flat migratory keratinocytes (14).

Therefore, keratinocytes from the wound edges and epithelial stem cells from hair follicles or sweat glands are activated and release different cytokines and growth factors. With the production of membrane-associated kinases, the permeability of the membranes increases – the signal for cells at the wound edges to retract and reorganize their intracellular tonofilaments in the direction of migration. Collagenases and elastases help loosening the intercellular desmosomes. Now keratinocytes are able to migrate by lamellipodial crawling along the fibrin blood clot in the higher layers of the granulation tissue until the cells touch each other and close the wound like a zipper (10).

1.2.3.2 Neovascularisation

The whole process of wound healing depends on sufficient supply with oxygen and nutrients. Thus, neovascularization is necessary. Growth factors, e.g. VEGF, PDGF, bFGF, bind to their receptors on the endothelial cells of existing vessels and activate signal pathways, so that the activated endothelial cells can secrete proteolytic enzymes to dissolve the basal lamina, enabling them to migrate into the wound. There, they release matrix metalloproteinases at the front of proliferation, to dissolve the surrounding tissue. This guarantees enough space for endothelial proliferation. Newly built endothelial sprouts form small tubular canals interconnect to others forming vessel loops (10).

The distinct pattern of neovascularization can be described forming a circle with an inner ring of circularly organized vessels directly at the wound border followed by radially shaped vessels supplying the inner ones and connecting to the vessels of the uninjured skin (14).

Throughout the healing process the inner loop shrinks, until the vascular ring has completely disappeared. Little by little the vessels differentiate into arteries and venules and mature by the recruitment of pericytes and smooth muscle cells, that stabilize the vessel wall. The initial blood flow marks the end of the angiogenetic process (10).

1.2.4 Granulation Tissue Formation and Tissue Remodeling

Granulation Tissue replaces the fibrin-/fibronectin-based provisional wound matrix and might produce a scar by maturation. A high density of fibroblasts, granulocytes, macrophages, capillaries, loosely organized collagen bundles and high vascularity are the main characteristics of granulation tissue, while a scar is avascular and acellular. With the production of collagen and ECM substances, fibroblasts are most important for building granulation tissue. At the end the number of maturing fibroblasts is reduced by myofibroblast differentiation and terminated by consecutive apoptosis (10).

The maturation of the wound may last up to 1 year, overlaps the proliferation phase and begins around day 7. Fibrin, fibronectin and thrombospondin-1 as well as other proteins are initially replaced by collagen type III. Over time, more and more collagen type I can be found. Thickening and orientation along stress lines correlates with intercollagen fiber connecting elements and increasing strength of the wound (9).

During the remodeling and maturation process the angiogenetic process diminish, the wound blood flow declines and the acute wound metabolic activity slows down and finally stops (10).

Myofibroblasts are important for wound contraction. Dermal fibroblasts, that were activated by growth factors, stimulated by mechanical tension and PDGF, turn into stress fiber-expressing protomyofibroblasts. These cells are found in early granulation tissue and in normal connective tissue with high mechanical stress. The protomyofibroblasts are activated by mechanical tension, activated TGF-β and the splice variant EDA fibronectin and differentiate into α-smooth muscle actin-expressing myofibroblasts. With their focal adhesion contacts between the intracellular cytoskeleton and the ECM they generate contractile forces to the wound (14).

1.2.5 Acute and Chronic Wounds

Wounds are commonly classified into 2 groups: acute and chronic wounds. Whilst acute wounds undergo the physiological wound healing process, chronic wounds are characterized by an insufficient repair process that precludes the establishment of a sustained anatomical and functional result in an appropriate length of time. They do no follow the stages of

physiological wound healing, but they are trapped in an uncoordinated and self-sustaining phase of inflammation. Although there is a huge variety of different factors causing chronic wounds, more than 80% are associated with venous insufficiency, high blood pressure or diabetes mellitus. Nevertheless, they show similar behaviour and progress, because of the multifactorial pathogenesis, including local tissue hypoxia, bacterial colonialization, repeated ischemia-reperfusion injury and cellular as well as systemic changes of ageing. Local tissue hypoxia leads to an impairment of mitochondrial oxidative phosphorylation with a reduced ATP production, so that a decrease of ATP-dependent membrane proteins, such as Na^{+}/K^{+}-ATPase or Ca^{++}-ATPase can be detected. The transmembrane potential subsequently gets lost and the cells start to swell. Calcium ions accumulate in the cells and activate signal pathways ending up in cell membrane disruption, leading to inflammation. Next to proinflammatory cytokines, endothelial cells express adhesion molecules that enhance the extravasation and invasion of neutrophils and macrophages, that show autocrine synthesis of proinflammatory cytokines, into the wound site (15).

In addition to this, chronic wounds show elevated levels of MMPs released from neutrophils and fibroblasts. Certain proteases have higher levels than their inhibitors, leading to an excessive degradation of growth factors and ECM components (15).

ROS are another key player in the development of chronic wounds. Produced by neutrophils and macrophages, chronic wounds show an imbalance between oxidants and antioxidants. This imbalance causes oxidative damage, e.g. proteins, lipids, DNA, and enhances expression of MMPs, serine proteases and inflammatory cytokines (15).

Another aspect, that triggers inflammation, is the colonialization of chronic wounds with bacteria (15).

Since most wounds occur in elderly (average age over 60), the healing response is basically and essentially delayed. Not only, that ageing cells show reduced viability and proliferative capacity, but also altered patterns of gene expression and a decreased response to growth factors. Independently to the patients' age, cells in chronic wounds also exhibit characteristics of premature senescence. This might probably be, because of stress factors such as chronic inflammation and the respective proinflammatory cytokines (TNF, TGF-β), the presence of ROS and the aggressive proteolytic milieu caused by bacterial infection and toxins (15). Epidermal hyperproliferation can also be detected in chronic wounds. Chronic wound edge keratinocytes therefore seem to express a gene signature reflecting partial proliferation activation, with several cell cycle genes, including cyclins, upregulated, but with a suppression of checkpoint regulators and p53 (16).

Acute versus chronic wounds (17):

Table 1: Characteristics of acute versus chronic wounds

Acute Wounds	Chronic Wounds
Low levels of bacteria	High levels of bacteria
Low inflammatory cytokines	High inflammatory cytokine levels
Low protease and reactive oxygen species levels	High protease and reactive oxygen species levels
Intact functional matrix	Degraded nonfunctional matrix
High mitogenic activity	Low mitogenic activity
Mitotically competent cells	Senescent cells

1.2.6 Risk Factors for Chronic Wounds

Chronic wounds can be the result of many different factors (18), local as well as systemic ones (17). The most important local ones are venous or arterial diseases, neuropathy, infection, necrotic tissue, excessive wound tension, unfavourable local environment, e.g. too dry/wet wounds, an inappropriate treatment, malignant wounds, radiation and repetitive trauma (17) (15).

Common systemic factors that can lead to chronic wounds are age, malnutrition, medications, especially corticosteroids and immunosuppressants, obesity, chronic medical conditions, e.g. diabetes, and habits like smoking or drinking alcohol (17).

The most common types of chronic wounds appear on the lower extremities and are the venous leg ulcers, arterial ulcers and the diabetic foot ulcers. The venous leg ulcers, mostly caused by chronic venous insufficiency, make about 50% to 70% of leg ulcers. The prevalence is 1% to 1.5%. About 25% of leg ulcers are arterial ones. They are mostly caused by atherosclerosis. In addition to this diabetes, smoking, hyperlipidemia, hypertension, obesity and an increased age are often associated with arterial leg ulcers. 4% to 10% of diabetes patients have to face diabetic foot ulcers, because of neuropathy and ischemia. About 60% of these patients also show signs of infection (17).

Next to the 3 most common types of ulcers, pressure ulcers from unrelieved pressure affect 1% - 5% of hospitalized patients. Therefore friction, moisture shearing forces and pressure itself are the main risk factors. Rare ulcer types can result from vasculitis, vasculopathy, necrobiosis lipoidica, pyoderma gangrenosum, malignancy-associated ulcers, hypertensive ulcers and a lot more (17).

1.2.7 Scarring

Next to normal scarring as a consequence of overgrowth of fibrous tissue after damage, injury or surgery (19), there are three different types of pathologic scarrings in humans, too: atrophic, hypertrophic scars and keloids. Atrophic scars form a valley or depression (20). Whereas keloids extend beyond the margins of the original tissue damage and do not regress spontaneously, hypertrophic scars develop within the margins and generally partially regress within 6 months. Histologically a different arrangement of collagen fibres, the presence of α-smooth muscle actin-positive myofibroblasts and an extent of angiogenesis are typical characteristics to differ between hypertrophic scars and keloids. Studies showed, that there exists common pathways of fibrosis (TGF-β, connective tissue growth factor, interleukins 4 and 13, PDGF, osteopontin) next to the tissue specific ones (16).

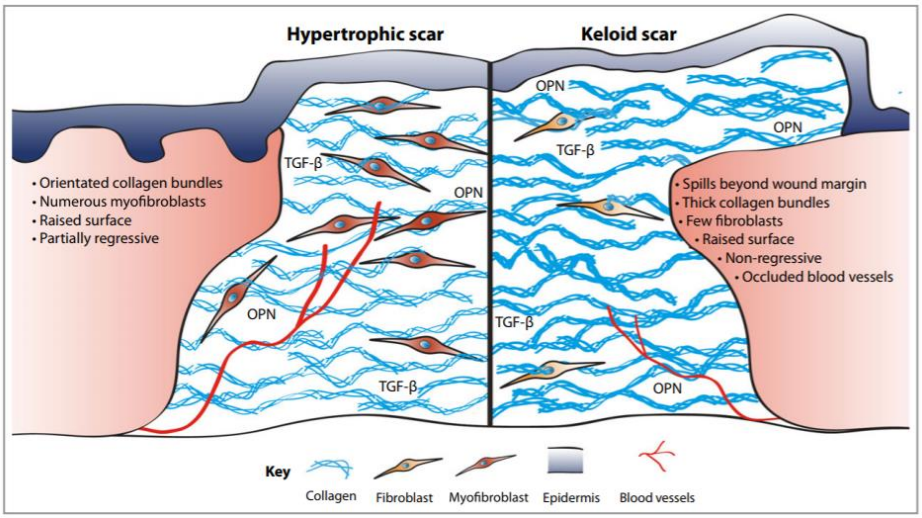

Figure 4: Hypertrophic vs. keloid scars
from (16)

1.2.8 Fetal Wound Healing

Healing without scarring is a speciality among the fetal wound healing process (21). In humans, the ability for scarless wound healing stops at approximately 24 weeks of gestation (10). At the moment, there are several hypotheses, why fetal dermis has the ability to regenerate a non-disrupted collagen matrix that is identical to the original tissue: differences in the ECM, the inflammatory response, cellular mediators, differential gene expression and stem cell function. Concerning the inflammatory response in embryonic wounds a lower number of less-differentiated cells and a very different profile of growth factors could be found. Molecular changes involve low levels of TGF-β1, TGF-β2 and PDGF and high levels of TGF-β3 (10) (22). Fetal skin is also rich in metalloproteinases, that promote scarless healing (8).

1.3 Current Models in Wound Healing Research

As a "representation of a real or actual object" as written in Oxford English Dictionary, models aim to clarify thinking, assist in the generation of hypothesis, and simplify complex problems, such as the wound healing process (23). However, every model has its limitations and therefore does not always reflect the actual pathology responsible (24).

In order to study the complexity of wound healing a variety of different wound healing models, including in-silico, in-vitro, in-vivo, ex-vivo, patient models and volunteer models, has been developed (25).

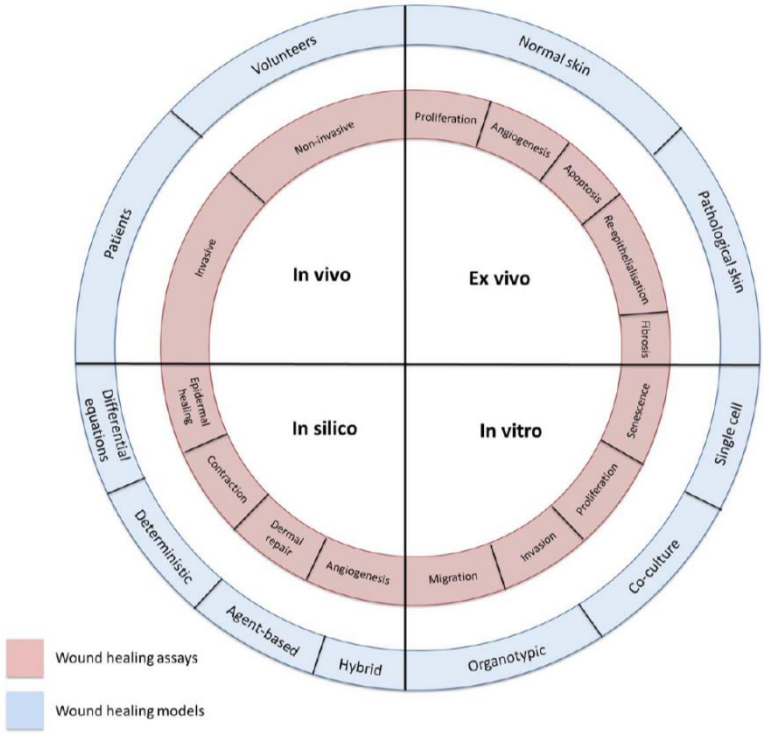

Figure 5: Main categories for human non-animal models of wound repair from (25)

Essential criteria for choosing the right model in research are the following (23):

- Accurate reproduction of the lesion
- The possibility for multiple investigations
- Exportability
- Ability to obtain multiple biopsy samples
- Compatibility with animal facilities
- Ease of handling
- Availability in more than one species
- Time required to obtain useful results

1.3.1 In-Silico Models

Computational models, also known as in-silico models, help to understand cell growth and to design efficient scaffolds and tissue substitutes. Over the years many different models have been developed to understand the complexity of the biochemical and biophysical processes. For example, with a number of different equations some models analyse strategies for improving healing as well as by the use of ordinary differential equations the effects of commercially engineered skin substitutes can be investigated. With multiphase models to describe time-dependent processes in vitro, agent-based models for understanding the role of growth factors, organisation of keratinocytes and a lot more, in-silico models may help for theoretical understanding and in combination with other models. Only the lack of physical characteristics of the human skin have to be considered (25) (26).

1.3.2 In-Vitro Models

For the study of the mechanism of action of a compound, which is complicated to observe in vivo, in vitro models can be used (23).

Single cell, co-culture and organotypic models are differentiated (25). In single cell systems, monolayers or three-dimensional cell matrices are commonly used. The relevant cells are grown directly on the plastic surface of culture dishes or other substrates e.g. collagen, fibrin (23). By scraping the dish surface and removing cells a scratch and trauma to the cells next to the "wound" is made. Cell proliferation, differentiation, protein production and secretion, viability, gene expression and migration can be studied (25).

Three dimensional matrices, e.g. fibroblasts, that are seeded in a type I collagen solution which is solidified to gel, allow the evaluation of cell contraction and matrix compaction (25). These 3D systems represent the normal wound physiology in a better way than 2D systems (23), but only one type of ECM protein and one cell type can be used (25).

To study cell interactions, e.g. keratinocyte-fibroblast interactions, co-culture or multicellular systems are appropriate, whereas organotypic models help to investigate scar pathogenesis and interactions between cells in a three-dimensional manner. In wound research keratinocytes are cultured separately and then placed on top of a collagen gel containing fibroblasts (25).

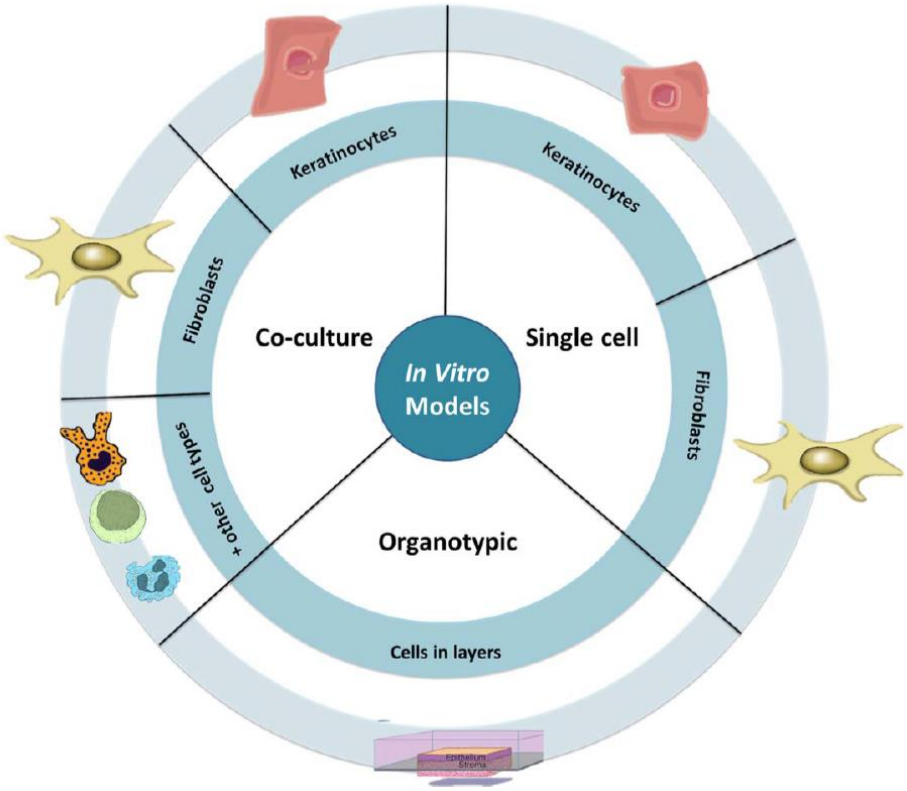

Figure 6: In-vitro models from (25)

Commonly used in-vitro models in wound research are the cell proliferation assay to determine if the number of cells in a culture is growing in presence or absence of a test substance, the cell cytotoxicity assay to determine if cells are killed by the presence of a test substance and the cell viability assay - a test to determine if cells are able to maintain viability when exposed to a test substance (24).

1.3.3 Ex-Vivo Models

When using whole skin biopsies in culture, human skin pathophysiology can be studied more adequately than in in vitro models. Ex vivo models can be classified into normal skin models, which use full-thickness or partial thickness skin, and pathological skin models. The latter are used when analysing stretch marks and scars. Mostly to develop new therapies, anti-inflammatory interleukin 10, anti-fibrotic streptolysin O and dermal substitutes, just to name a few, have been evaluated by ex vivo models (25).

1.3.4 In-Vivo Models

Since using in silico, in vitro and ex vivo models only provides information about particular processes in wound healing, in vivo models are needed for more accurate understanding of

the whole regeneration process of human skin, including cell interactions, biochemical processes and growth factors.

1.3.4.1 Animal Models

Animal models are essential for basic research and development, although they do not always accurately represent the structure of human skin or develop similar scars (25).

However, is it all about anatomy and physiology of the skin, that influences the wound healing process the most. Nevertheless, animal models are used to study wound healing basics and to analyse complex correlations. With the identification of the same mechanisms in wound healing as in humans, more in-depth investigations and experimental manipulations could be established (24).

Rodents are commonly used for the basis of wound healing studies, since they are available, low cost and easy to handle, although their wound healing process is completely different from that of humans (24).

To simulate human wound healing, porcine cutaneous models seem to currently be the best option (27). Not only that their anatomical structure is quite similar to human skin, but the physiological reaction to trauma is nearly the same (24).

1.3.4.2 Human Models

Human models are necessary to generate clinically relevant experimental data (24). The pathology and physiology of healing in patient or volunteer models is the same as in patients (25).

The patient model is not only useful to validate potential novel wound and scar therapies, but also to assess different wound types using incisions, excisions and biopsies. Volunteer models are quite limited and do not allow to create abnormal wounds or pathological scars. Although, different wound models for human volunteers exist, as shown in table 2 (24):

Table 2: Human skin models

Wound model	Depth into skin
Skin stripping using adhesive tape	Stratum corneum
Suction Blister model	Epidermis A split in the basal membrane produces a clear removal of the epidermis with the dermis remaining 100% intact
Abrasive wound model	Epidermis As the dermis provides greater resistance to the brushing only epidermal cells are removed
Laser wounds	Variable depth depending on laser type and energy settings. Lasers can be tuned to induce very superficial i.e. just upper epidermal layers to deeper wounds, i.e. full epidermis and partially dermis
Microdermabrasion	Variable depth depending on device and device setting
Dermatome	Split-thickness wounds This will remove 100-1500-micron-thick layer of the epidermis/upper dermis
Biopsy	Full thickness wound model Removal of epidermis and dermis. Depth depends on biopsy technique, i.e. punch vs. scalpel

1.4 The Chick Chorioallantoic Membrane (CAM) Assay

Being superior to classic in-vitro models, the chick chorioallantoic membrane not only represents a common alternative to animal testing but does not raise ethical or legal questions or violates animal protection laws (2). Furthermore, because of the lack of innervation during the respective timeframe of embryonal development no pain can be experienced (28). According to the Institutional Animal Care and Use Committee (IACUC) and the National Institutes of Health, USA, a chick embryo that has not reached the 14th day of its gestation period would not experience pain and can therefore be used for experimentation (29).

In Europe, the European Partnership for Alternative Approaches to Animal Testing (EPAA), also promotes methods, according to the 3R principle (reduction, refinement and replacement of laboratory animal use) to reduce animal testing (30).

One of the first descriptions of the usage of CAM assays in research dates back to 1938, when Ernest W. Goodpasture et. al. worked on 'A Study of Human Skin Grafted upon the Chorio-Allantois of Chick Embryos' at the Department of Pathology and Surgery in Nashville (31). Since then the CAM Model became more and more popular in research, especially for the studies of angiogenesis and tumorigenesis (32) (33) (34).

The chick chorioallantoic membrane is an extraembryonic membrane, which is responsible for gas exchange. As the surface of the noncellular eggshell membrane, it is formed by the fusion of the splanchnic mesoderm of the allantois and the somatic mesoderm of the chorion. On day 4 of incubation, the CAM starts to develop. An extensive network of extraembryonic capillaries forms and covers the whole surface by day 12. Respiratory and excretory function – two physiological functions – are implemented with these vessels (35).

Another specific characteristic is the lack of the immune system. Studies indicate, that T- and B-lymphocytes start to appear at day 11, but do not become mature until hatching on day 21 (28). For this reason, the chick embryo serves as a naturally immunodeficient host capable of sustaining grafted tissues and cells without species-specific restrictions (32).

For better handling in research Deryugina et.al refined an ex-ovo culture method. Until this point in time, CAM experiments were carried out in-ovo, by cutting a window through the egg shell. The ex-ovo method allows better accessibility of the CAM and chick embryo as well as better in-vivo documentation and manipulation of the embryo (32) (36).

The idea of using the chick chorioallantoic membrane assay as an in-vivo xenograft model for human skin has been known for quite some time. Goodpasture et al. engrafted human skin to the chick CAM and published the method as one of the first in "A study of human skin grafted upon the chorio-allantois of chick embryos" in 1938 (37) (31).

It could be demonstrated, that within a few days the vessels of the developing CAM fuse with those of the skin, keeping the skin viable and healthy for up to 9 days. (37)
Furthermore, Kunzi-Rapp et. al. transplanted human skin to the CAM and tested different substances on it after 5 days of engrafting (37). In addition to this the CAM can also be used to test anti-cancer drugs (29).
In "The human skin/chick chorioallantoic membrane model accurately predicts the potency of cosmetic allergens" by Slodownik et. al. another human skin-CAM model was used for testing for allergenicities (37).

1.5 Skin Grafts

Depending on the depth of skin harvested (38), a classification between epidermal grafts, full-thickness and split-thickness skin grafts can be made. Epidermal grafts only consist of the epidermal layer of skin (39), whereas full-thickness grafts consist of the whole epidermis and dermis with associated adnexal structures. In contrary, split-thickness grafts contain the entire epidermis but only part of the dermis and associated adnexal structures (40).

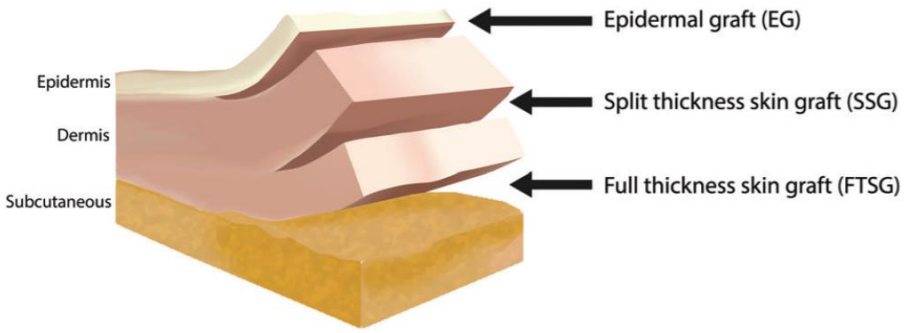

Figure 7: Overview of skin grafts
from: (39)

1.6 Rose Bengal

Rose bengal - 4,5,6,7-tetrachloro-2',4',5',7'-tetraiodofluorescein - is a halogenated xanthene dye. It is mostly used as a photosensitizer in biological and non-biological systems (41). After activation by illuminating it with green excitation light Rose bengal generates radical oxygen species (ROS) (42).
Studies show, that in absence of oxygen efficient electron transfer can be detected between Rose bengal and biological donor molecules as well as with Rose bengal ground state, when concentrates are high. This electron transfer produces semi-oxidized radicals and the semi-reduced radical Rose bengal^{3-}. In aqueous solution Rose bengal dissolves without a change

in the absorption spectrum and by sequential loss of iodines tetrachloro-fluorescein is produced (41).

1933 Sjogren was one of the first to describe a unique Rose bengal staining pattern in patients with keratoconjunctivitis sicca, making it become popular for usage in ophthalmology. In the 1960s a study by Norn showed, that Rose bengal stains dead or degenerated cells, but not healthy ones (43). Therefore it is nowadays allowed to stain corneal surface damage. Furthermore it had been used as a diagnostic for liver function (41).

Rose bengal has also been used in many mouse and rat studies to induce photothrombotic cortical lesions (44) (45) (46) (47).

1.7 Aim of the Study

Since the prevalence and incidence of chronic wounds is increasing (1), it is important to study the role of ischemia in human wound healing. Inflammation and ischemia play the main role during regenerative processes after damaging. In-vivo models in wound healing research may be the best options available with regards to the similarity in the whole regenerative process. However, it is not yet possible to only study the influence of ischemia. This is because of the inflammation process that starts immediately after injury and dominates the affected area.

We aim to develop a new model, where it is possible to induce ischemia in selected areas with human split skin, without activating inflammation. This enables researchers to observe changes e.g in angiogenesis, cell proliferation only based on the influence of the ischemia state. Due to that our model could also be used to test new substances and develop new therapies for chronic wound treatment.

Our study was approved by the ethics committee of the Medical University of Graz, prior to the implementation.

2 Material and Methods

The following timelines show the planned chronological sequences of the project. The main steps are highlighted with block arrows. In the “first series” of experiments no skin grafts were transferred onto the CAM. It was just used for studying Rose bengal induced photothrombosis. In the “second series” of experiments split skin grafts were transferred on day 7. After they had been completely integrated in the CAM, ischemia was induced on day 11. Both series were planned to be stopped on day 14 of chicken embryonic development.

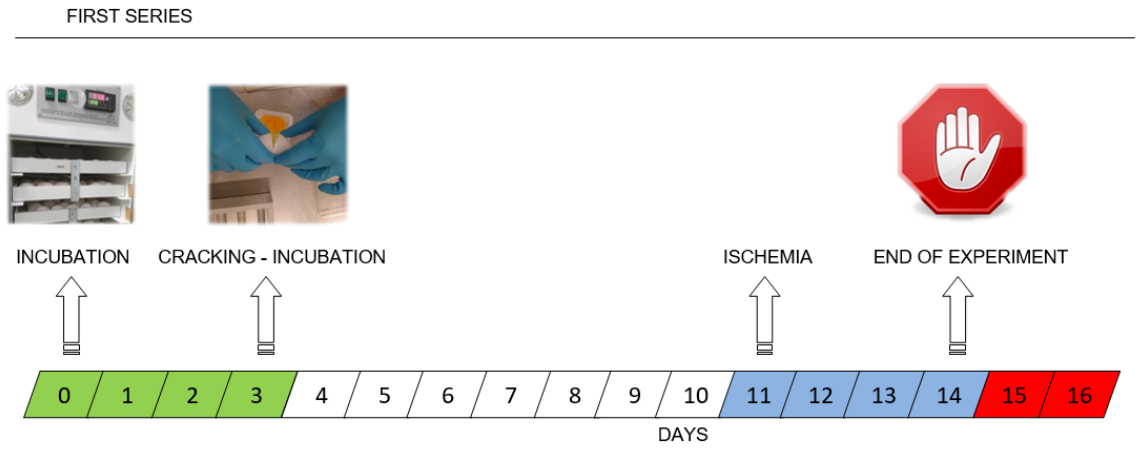

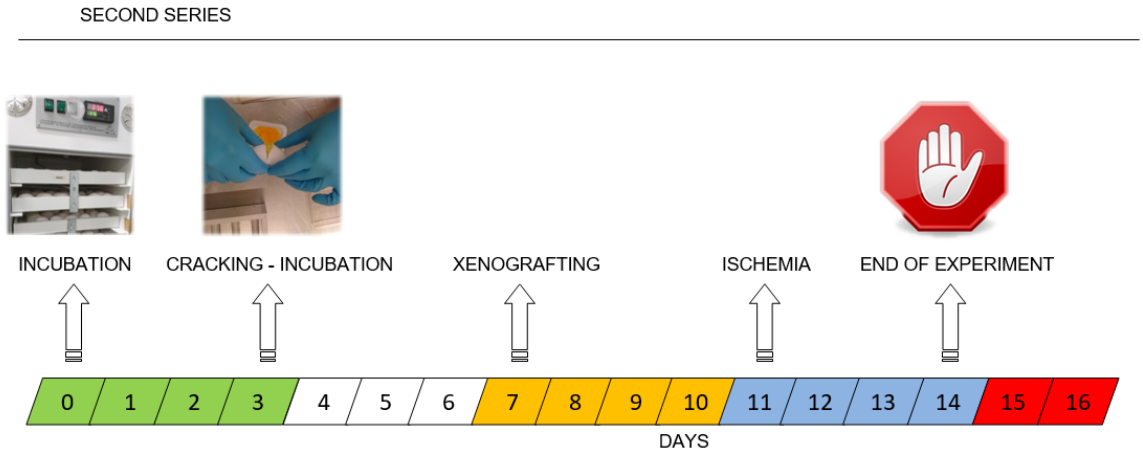

2.1 Chick Chorioallantoic Membrane (CAM) - Assay

For all the experiments fertilized white Leghorn eggs from a local hatchery in Gloggnitz, lower Austria, were used.

110 eggs had to be washed at the right temperature and visible contamination was removed with a brush. After drying, 75% EtOH was sprayed all over them to ensure sterile conditions. Then the eggs were put into the incubator at 37.6°C and 40-60% humidity for 3 days. During this time they got automatically turned, what is necessary for embryonic development.

2.2 Preparation of the CAMs

2.2.1 Cracking Process

Material:

- Sterile Scales Pans
- Sterile Square Petri dishes
- UV Box-E2/40H-NX-R (Light Progress UV Ray Technology)
- Angle Grinder
- 75% EtOH
- 75% Ethanol bath
- Container for unfertilized or dead eggs
- Container for eggshells

The scales pans and square petri dishes have to be prepared the day before cracking. Therefore it is used to immerse them in a 75% ethanol bath and put them afterwards into an UV sterilizer. In our lab we used the "Light Progress UV Ray Technology Sterilizer", which guarantees a sterilization rate of 99,99% after a 16 minutes usage.

On incubation day 3 of the eggs, the cracking process was performed. After sterilisation of the laboratory space with 75% EtOH, the whole equipment was prepared. Figure 8 shows the lab space.

Figure 8: Cracking equipment

The eggs were taken from the incubator and were put into a 75% EtOH bath with their underside, shown in Figure 9 to reduce infection risk while doing the cracking process.

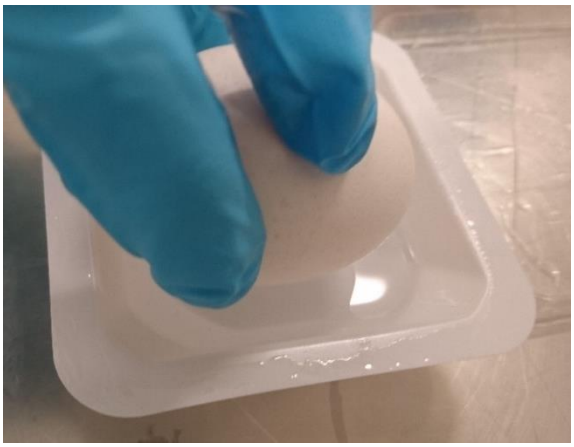

Figure 9: 75% EtOH bath

It is crucial, that the eggs are not turned around anymore after they are taken from the incubator. This is to make sure, that the embryo is located on the upper side of the egg and that it will not get injured during the opening process of the eggshell.
With a small angle grinder we created a 0.5 to 1.0 cm cut on the underside of the egg (Figure 10 A, B).

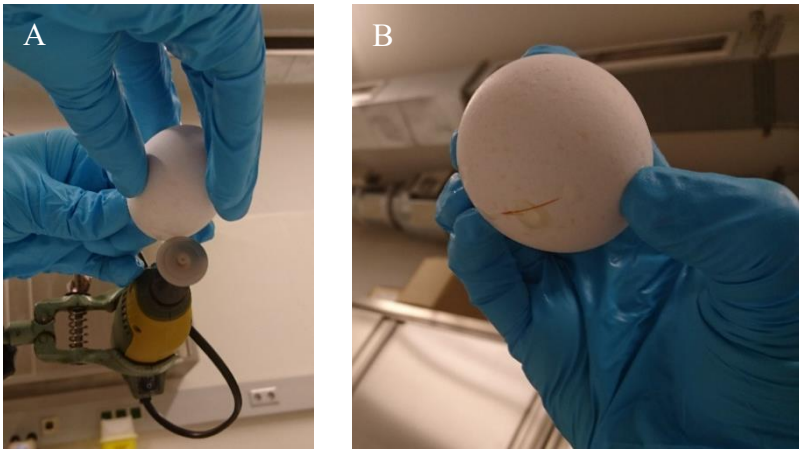

Figure 10: Egg opening

Then the egg was slowly put into a sterile scales pan, with the cut pointing downwards. While carefully exerting pressure with the thumbs from the upper egg's surface and a minimal rotation of the egg in the scales pan it is possible to create a straight fracture of the eggshell, to open it and to transfer the embryo from in-ovo to ex-ovo (Figure 11 A-C)

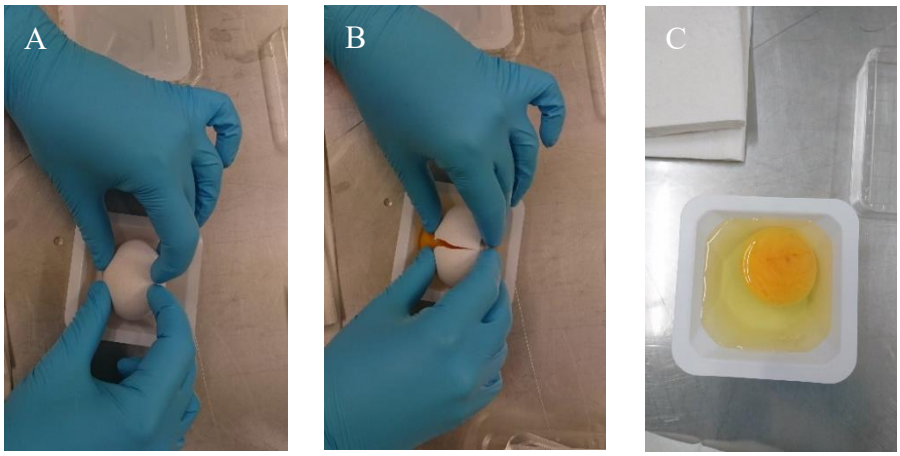

Figure 11: Cracking

In this state one can easily differ between living and dead embryos by visual control. A heartbeat as well as a primitive vessel system prove viability.

In the end sterile square petri dishes were used as covering (Figure 12) and the ex-ovo Embryos were put back into the incubator for 7 days at 37.6°C and 40-60% humidity. During this time the coverings were regularly opened to ensure sufficient oxygen supply.

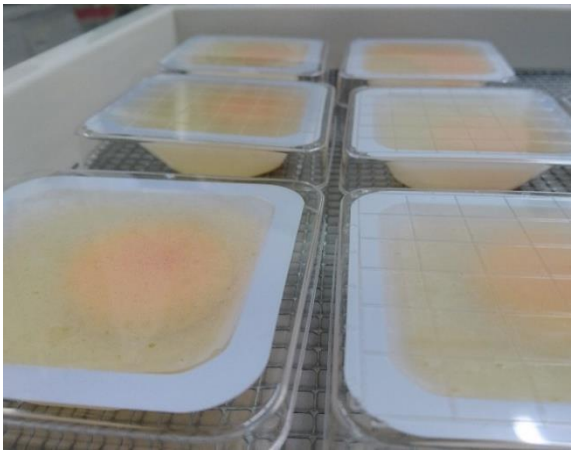

Figure 12: Ex-ovo systems

2.3 Split Thickness Skin Graft Transplantation

The split thickness skin used in the experiments was taken from a 53-year old female patient from the Division of Plastic, Aesthetic and Reconstructive Surgery, LKH Univ.-Klinikum Graz undergoing abdominoplasty. The split thickness skin was harvested from the resected skin portion at 1/10 mm thickness with an electric dermatome. The patient was informed about the usage of her skin for research beforehand and had signed the informed consent form.

Within 1 hour after the removal, the split skin grafts were stored in phosphate buffered saline at 5°C and transported to the Institute for Pathophysiology and Immunology.

Skin samples were produced of the sheets using a 5mm biopsy punch. The samples were directly transferred to the CAM of 7 days old chicken embryos. On every CAM two split-thickness skin samples of 5mm diameter with the dermis in contact with the chick tissue were placed in a distance of at least 2cm, since after the injection of Rose bengal, one of the grafts would be illuminated by a cold light lamp using a 525/50nm filter, whereas the other one would serve as a reference in the non-illuminated area of the CAM to show that without illumination, no photothrombosis can be induced.

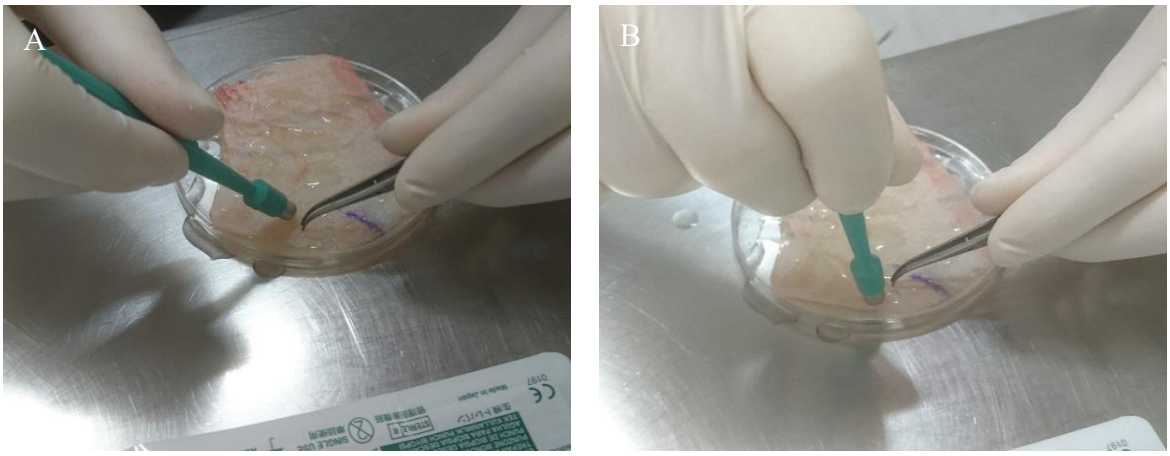

Figure 13: Biopsy punches (5mm) to produce split thickness skin samples

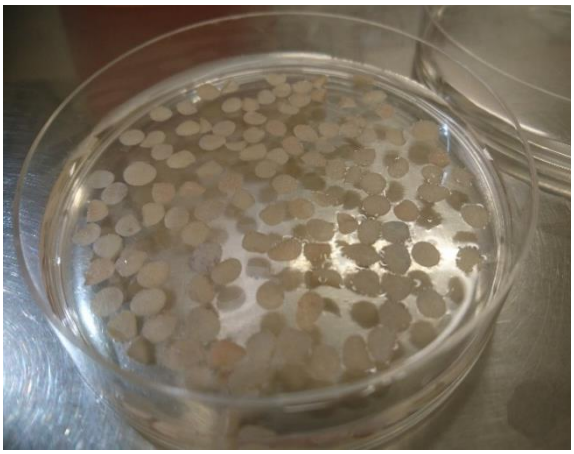

Figure 14: Split thickness skin samples

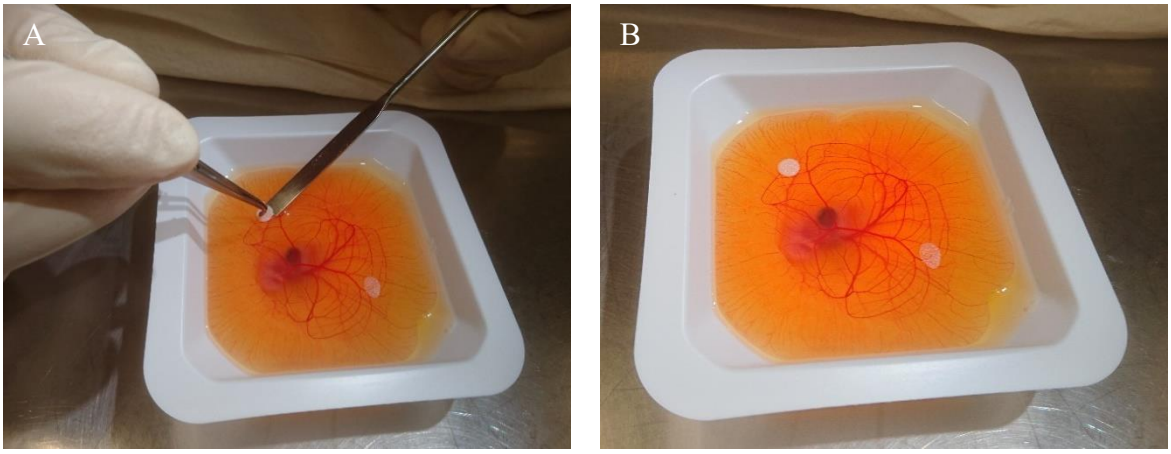

Figure 15: Split thickness skin grafting process

After placing the split skin grafts on the CAM, the embryos were put back into the incubator for 72 to 96 hours to permit engraftment. Viability of the engrafted skin fragments was determined by the normal colouration and texture of the skin indicating vascularization by the host and by the typical distribution of CAM blood vessels radiating out from the graft (37).

Eight representative CAMs were documented on the day of transplantation (day 7 of incubation) and 72 hours, shown in Figure 16-18.

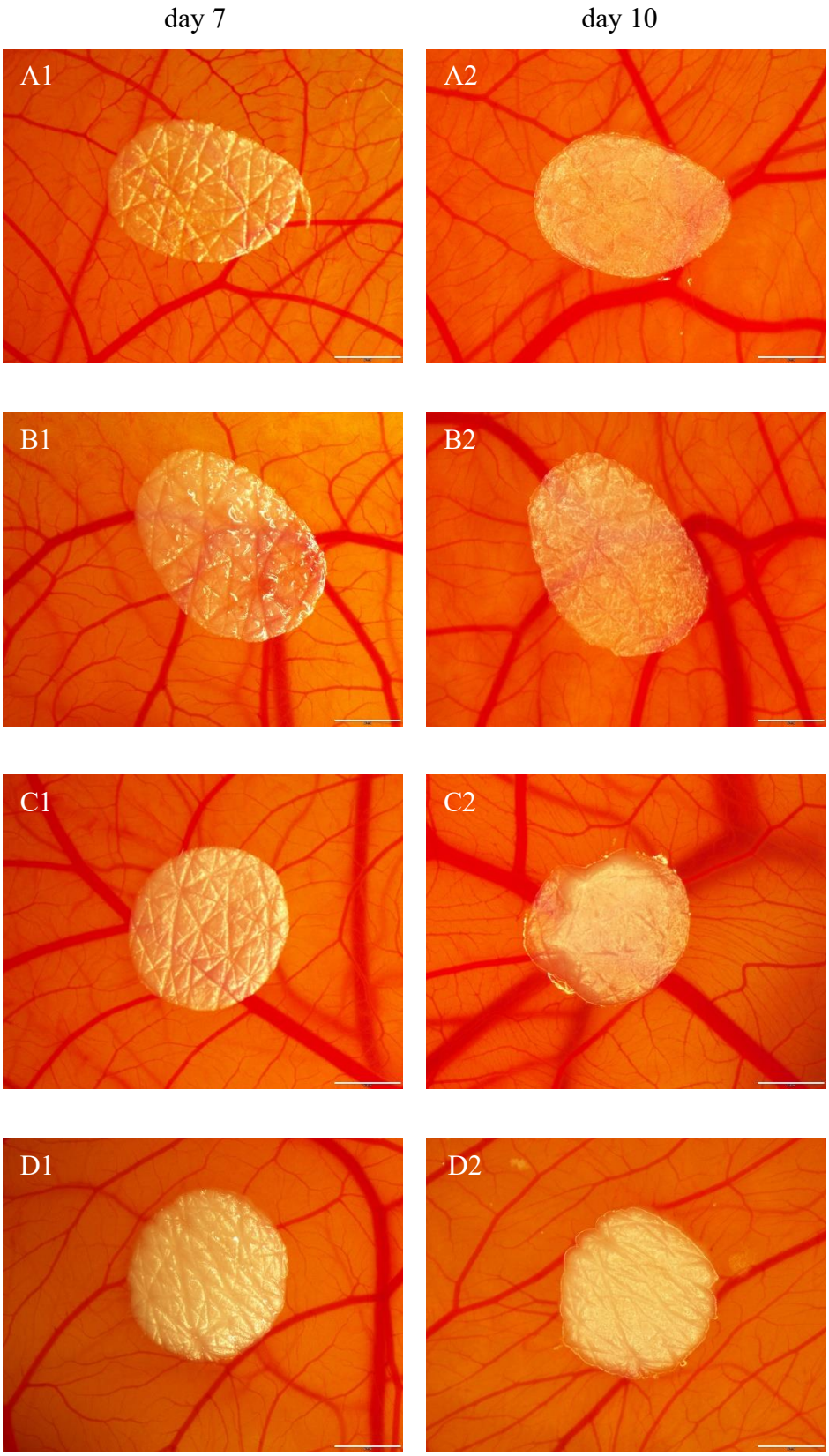

Figure 16: Split skin day 7 (viable) versus day 10 (viable) after transplantation 1

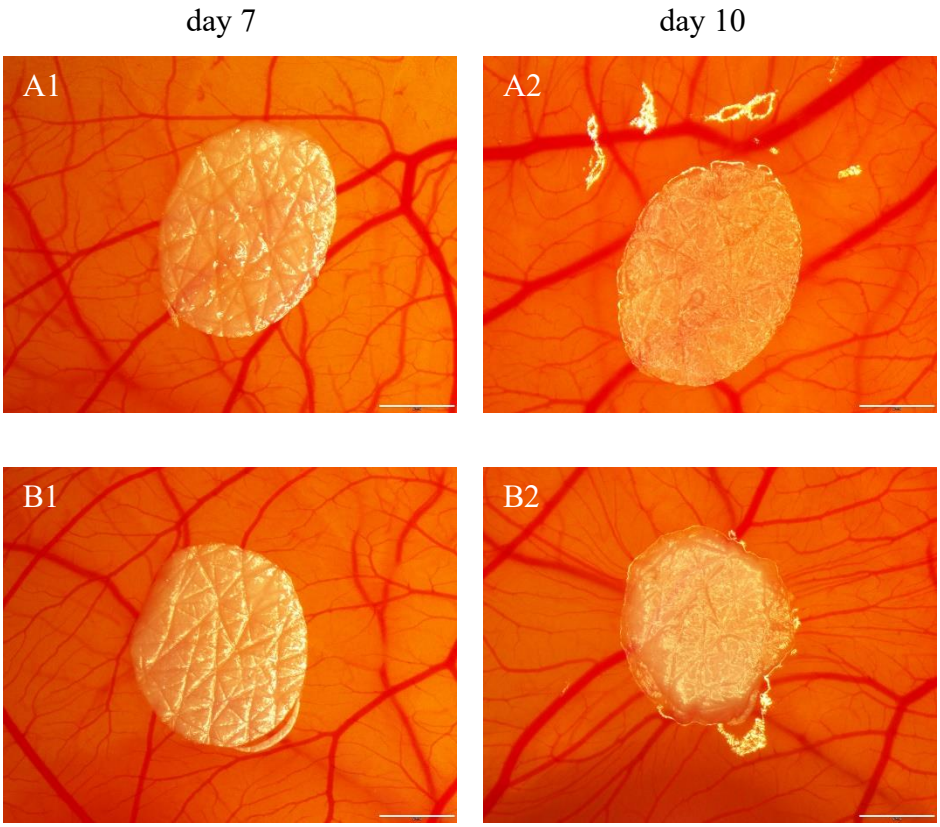

Figure 17: Split skin day 7 (viable) versus day 10 (viable) after transplantation 2

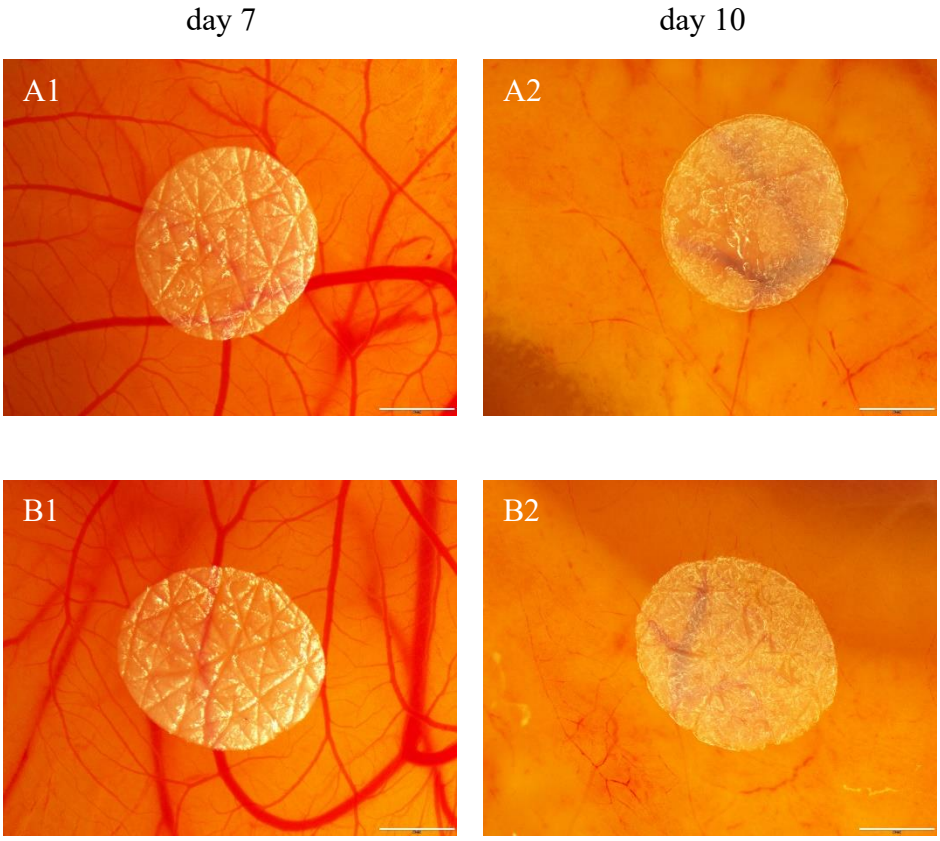

Figure 18: Split skin day 7 (viable) versus day 10 (non-viable) after transplantation

2.4 Glass Micropipette Pulling

For the injections of Rose bengal special glass micropipettes had to be pulled. Therefore we used the “Flaming/Brown Micropipette Puller Model P-1000” from Sutter Instruments.

The following settings were adjusted:

- Ramp: 511
- Heat: 520
- Pull: 0
- Velocity: 28
- Time: 200
- Pressure: 600

Specification of the used glass capillaries:

- Manufacturer: Harvard Apparatus Ltd.
- Standard Wall Borosilicate with filament
- Harvard: 30-0060
- Clark description: GC150F-7.5
- Glass size (OD x ID x length): 1.5mm x 0.86mm x 75mm

Method of pulling the glass micropipette:

The glass capillary is slightly fixed in the intended position of the micropipette puller on one side as shown in figure 19.

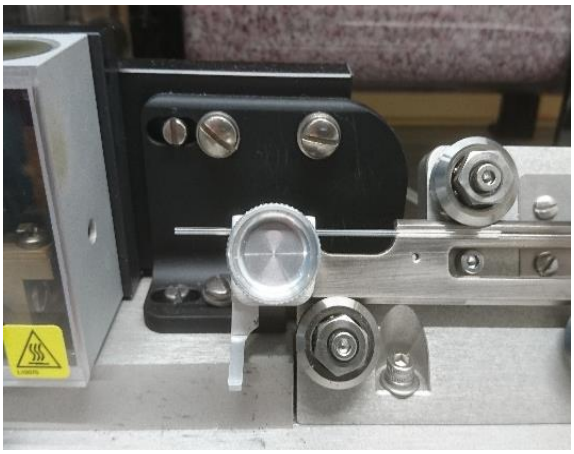

Figure 19: Fixing the glass capillary

Then the glass capillary has to be slid through the heating coil carefully and fixed on the other side in the same way and the pulling process can be started (Figure 20).

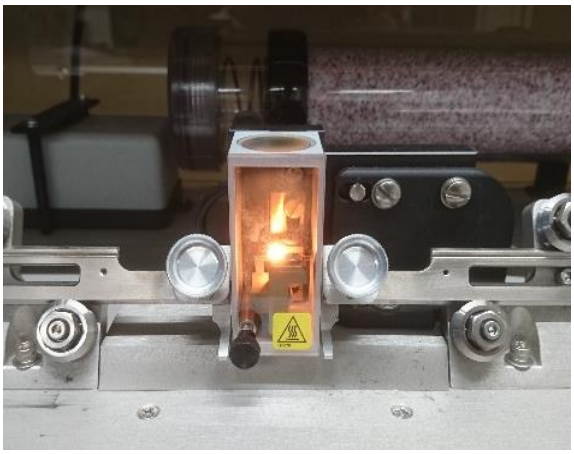

Figure 20: Heating and micropipette pulling process

When the programme has finished, two micropipettes can be taken out of the micropipette puller (Figure 21 A, B).

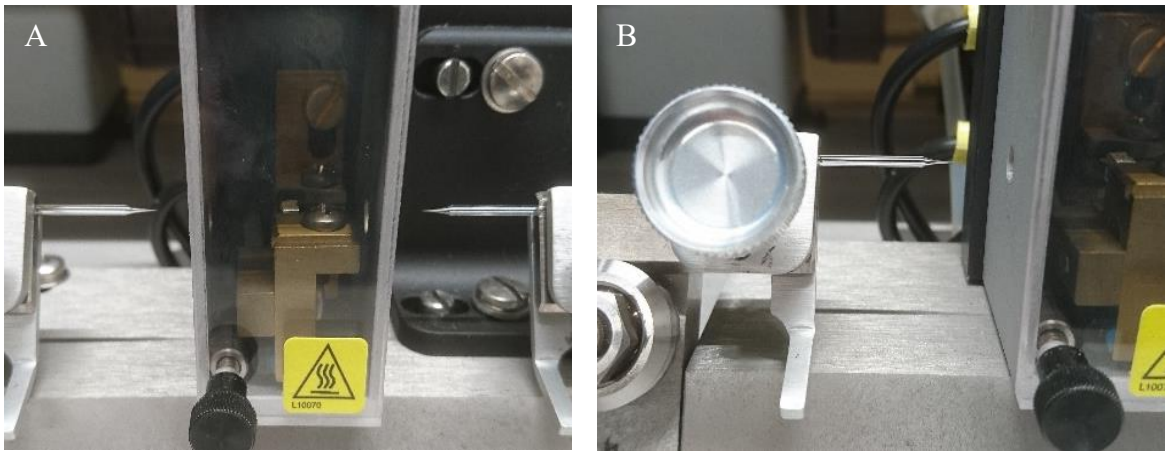

Figure 21: Pulled micropipettes

2.5 Rose Bengal induced Photothrombosis

2.5.1 Concentration of Rose Bengal in CAM

Rose bengal has never been used in the CAM assay before. Therefore the correct concentration of Rose bengal had to be calculated for our experiments initially. As all the concentrations in mouse and rat models are based on the animal's weights, the weight of the embryos and the chorioallantoic membrane (excluding the egg white and the yolk sack) was assessed for further calculation. Since we injected Rose bengal at day 11 we weighed five 11 days old chicken embryos.

At first the embryos were cooled down on crushed ice in their scales pans. Then the chorioallantoic membrane was carefully stripped off from the edges of the scales pans and from the yolk sac using a tweezer. With the help of a second tweezer the embryo and the chorioallantoic membrane were both lifted and transferred into a new scales pan. After weighing, the dead embryos were frozen and properly disposed.

Results:

Scales pan:	2.35g
Embryo 1*:	4.50g
Embryo 2*:	4.37g
Embryo 3*:	4.15g
Embryo 4*:	4.26g
Embryo 5*:	4.45g

The arithmetic means of the weight of 5 embryos including their CAM is 4.35g. This was taken as the reference for calculating the concentration of Rose bengal for injection on day 11 of incubation.

*Weight includes Embryo and the chorioallantoic membrane on day 11. Since the chorioallantoic membrane is rich in blood vessels, in which Rose bengal is distributed after injection, too, it was taken into consideration for the calculations.

2.5.2 Calculations of Rose Bengal Dosage for CAM

For the calculations of the right dosage in CAM the scientific work "Photothrombotic ischemia: a minimally invasive and reproducible photochemical cortical lesion model for mouse stroke studies" from Vivien Labat-gest et. al.

In the paper it is written that for the right amount of Rose bengal they *"injected 10 µl/g animal weight in female CD1 mice 12 weeks old in the present protocol. The amount of Rose bengal needed to produce the desired cortical lesion size can be easily determined in a separate set of preliminary experiments by testing different dosages (typically 2 µl/g, 5 µl/g or 10 µl/g body weight). Note that the amount of Rose bengal to be injected is highly dependent on the experiment conditions, particularly the type of light source used and the duration of light exposure. In the present study, 10 µl/g (150 µg/g) dose was found to be necessary to induce photothrombosis upon exposure to light for 15 min, whereas other groups reported that either 50 µg/g 6,8 and 100 µg/g10 intraperitoneal injection was sufficient for inducing a photothrombotic lesion."*

In "Thrombus formation induced by laser in a mouse model" by Pérez et. al. it is written that "*various concentrations (5,10,25 and 50mg/kg) of rose bengal were administered*" (48).

Our calculations are therefore based on these papers.

2.5.3 Preparation of Rose Bengal, Dosages for CAM and Process of Injection

Material for Rose bengal solution:

- Phosphate buffered saline
- Rose bengal
- Test tube

Material for injection:

- Sterile glass capillaries
- Pipettes
- Eppendorf tubes
- Tweezer
- Injection system
    - made of plastic tubes with a filter inside for sterile conditions
- Fibrin adhesive spray
- Microscope system
    - We used an Olympus Stereo Microscope with an X-Cite 120 PC Fluorescence Light Source (120 W) and Fluorescence Filter Cubes

All preparations were done under sterile conditions:

1. A solution of Rose bengal in phosphate buffered saline with a concentration of 100mg/ml was prepared. Therefore we weighed 131mg of Rose bengal and dissolved it into 1.3ml of PBS.
2. Three dosages were tested:
    a. 25µl/g: inject 1.1 µl of the solution
    b. 50µl/g: inject 2.2 µl of the solution
    c. 75µl/g: inject 3.7 µl of the solution

3. The right amount of solution was drawn up a pipette and transferred it into an Eppendorf tube.

4. A glass capillary was taken and put with the bottom end in the Eppendorf tube, so that the solution can move up the capillary by cohesion and adhesion.

5. The filled glass capillary was put in the injection system and the ideal blood vessel with a diameter of about 40-80µm (42) was chosen.

6. The next steps had to be done under the microscope. With the help of a tweezer, the CAM next to the vessel was carefully lift and fixed while the vessel was punctured with the glass capillary

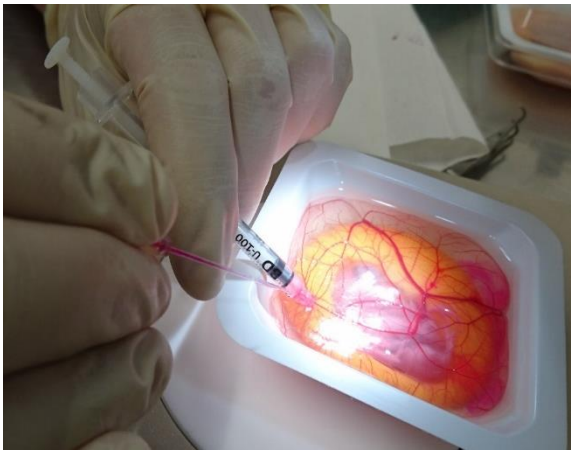

Figure 22: Injection process

Figure 22 shows the injection process. Next to the right vessel, the CAM was fixed with the help of e.g. a syringe by applying a vacuum, before the vessel was punctured with the glass capillary.

7. The solution was slowly injected by blowing air from the mouth into the injection system.

8. To stop bleeding oxidized cellulose as described in 2.7. was used. Just a little piece of it stopped the bleeding immediately and did not influence the CAM.

9. It took about 5 seconds until the solution of Rose bengal was distributed in the whole vascular system of the chicken embryo and CAM.

10. A cold light illuminator with a wavelength of about 549 nm - the absorption peak of Rose bengal – and 120W power was used.

11. The chosen vessel was then illuminated for 10 to 20 min.

In our experiments a visible clot was formed after seconds of illumination when given 2.2µl of a solution of 50mg/ml concentration.

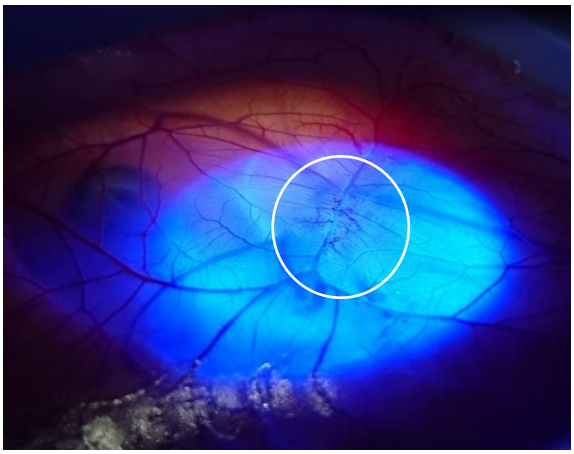

Figure 23: Macroscopically visible changes of the vessels

While illuminating the CAM structural changes of the blood vessels could be detected. In Figure 23 they are marked with a white circle.

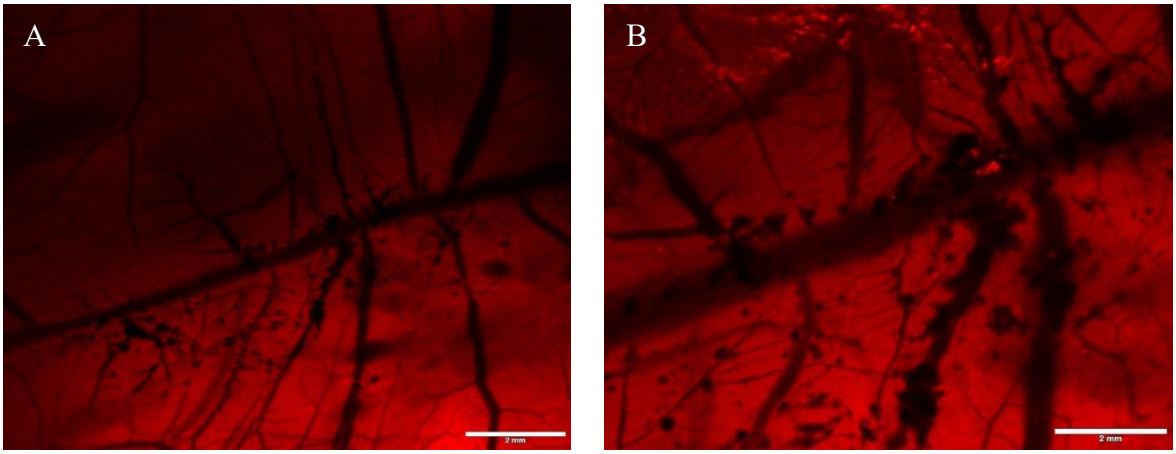

Figure 24: Stable clots of thrombosis

Figure 24 shows stable clots along the vessels, especially along the capillaries, next to the injection site, where there the focus of illumination was. This phenomenon could be seen during the pretests when trying different dosages.

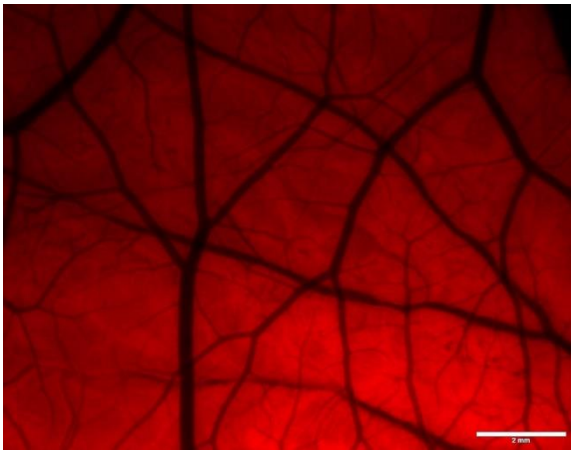

Figure 25: Untreated CAM vessels

Figure 25 shows the vascular system of an untreated CAM Assay. In comparison to the assay with injected Rose bengal, no visible changes of the blood vessels could be detected.

2.6 Method of Stopping Bleeding

After the injection process, there used to be a more or less significant bleeding. Experiments showed, that even the tiniest amount of blood loss (a few millilitres), could lead to immediate death of the developing chicken embryo.

Since no research data about how to stop bleeding in CAM vessels could be found, different approaches to achieve hemostasis were tried. For adequate hemostasis following criteria were defined:

1. Stop bleeding within seconds
2. Can be used in CAM
3. Can be removed afterwards
4. Breathable material, so that the CAM area will not get further reduced
5. No toxicity
6. No active substance, that will influence the vessel system or the chicken embryo

For the experiments oxidized cellulose, also known as m-doc, was used in form of little sponges which are commonly used for first aid in epistaxis. The sponges do not stick to the mucous membranes, stop bleeding within seconds of application, prevent new bleeding after removal, are permeable to air and hypoallergenic.

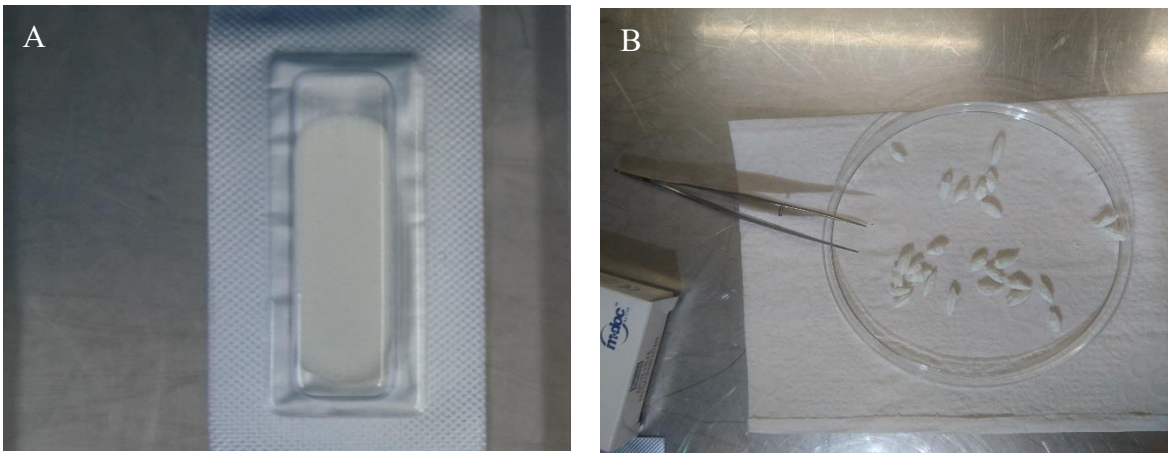

Figure 26: Oxidized cellulose

Figure 26, A shows the sponge-formed oxidized cellulose that we just cut into little pieces of about 0.8 mm as shown in Figure 26, B. These little pieces could be taken with a tweezer and pressed onto the bleeding vessel right after injury.

A step by step documentation of our method is shown in Figure 27 A-E.

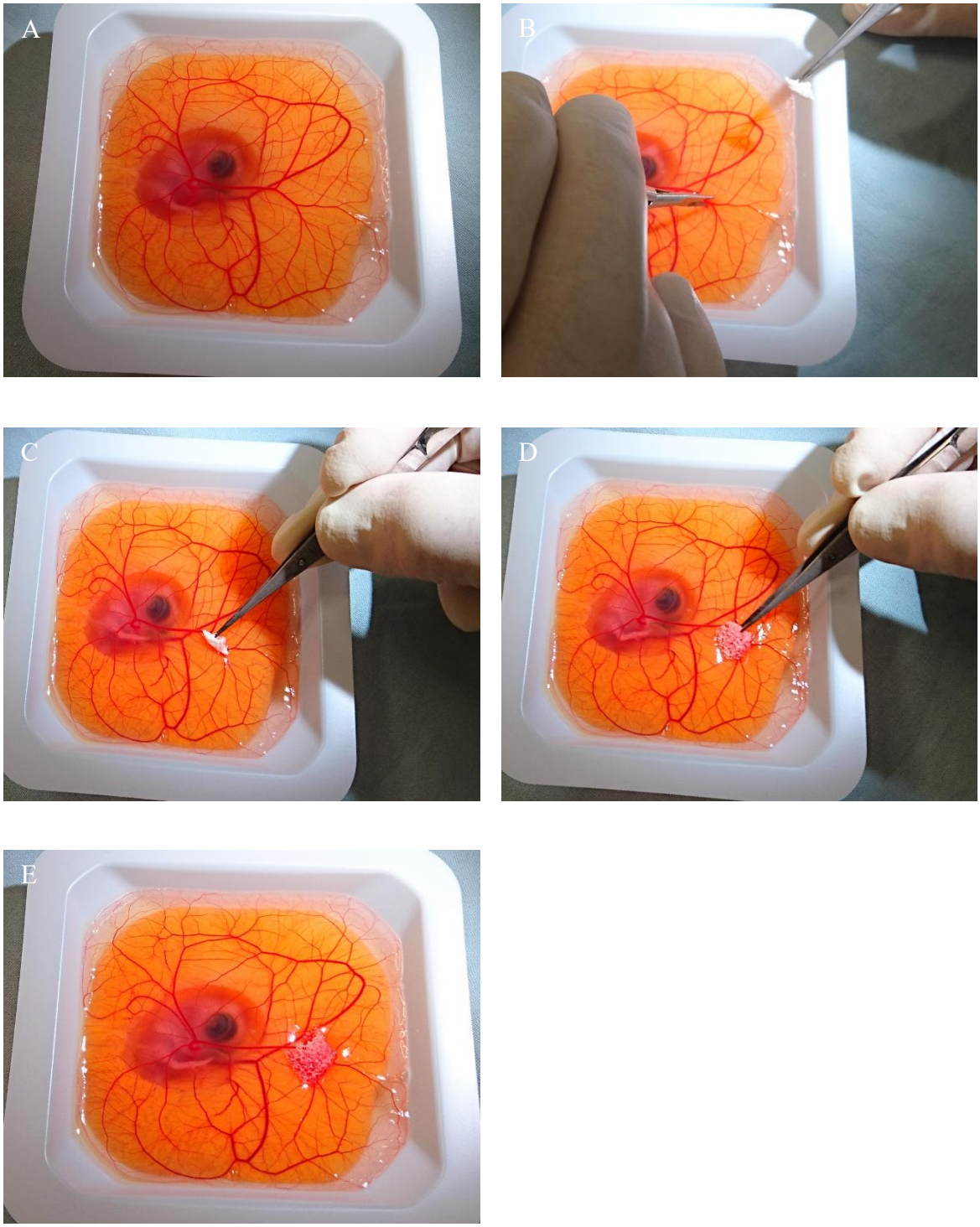

Figure 27: Blood stopping method - step by step

To show the efficiency of our method we cut through the whole vessels – for greater trauma and bleeding – of day 10 old chicken embryos with a scissor. Right afterwards one of the little sponges was pressed onto the two endings of the vessel for about 30 seconds. During the first 2-10 seconds, depending on the intensity of bleeding, the sponge not only absorbed the blood, but also unfolded, became bigger in size and sealed up the whole area, while

stopping the bleeding during the first seconds of contact. Figure 28 A-D shows another example of it with special focus on the changes of the sponge during the first seconds.

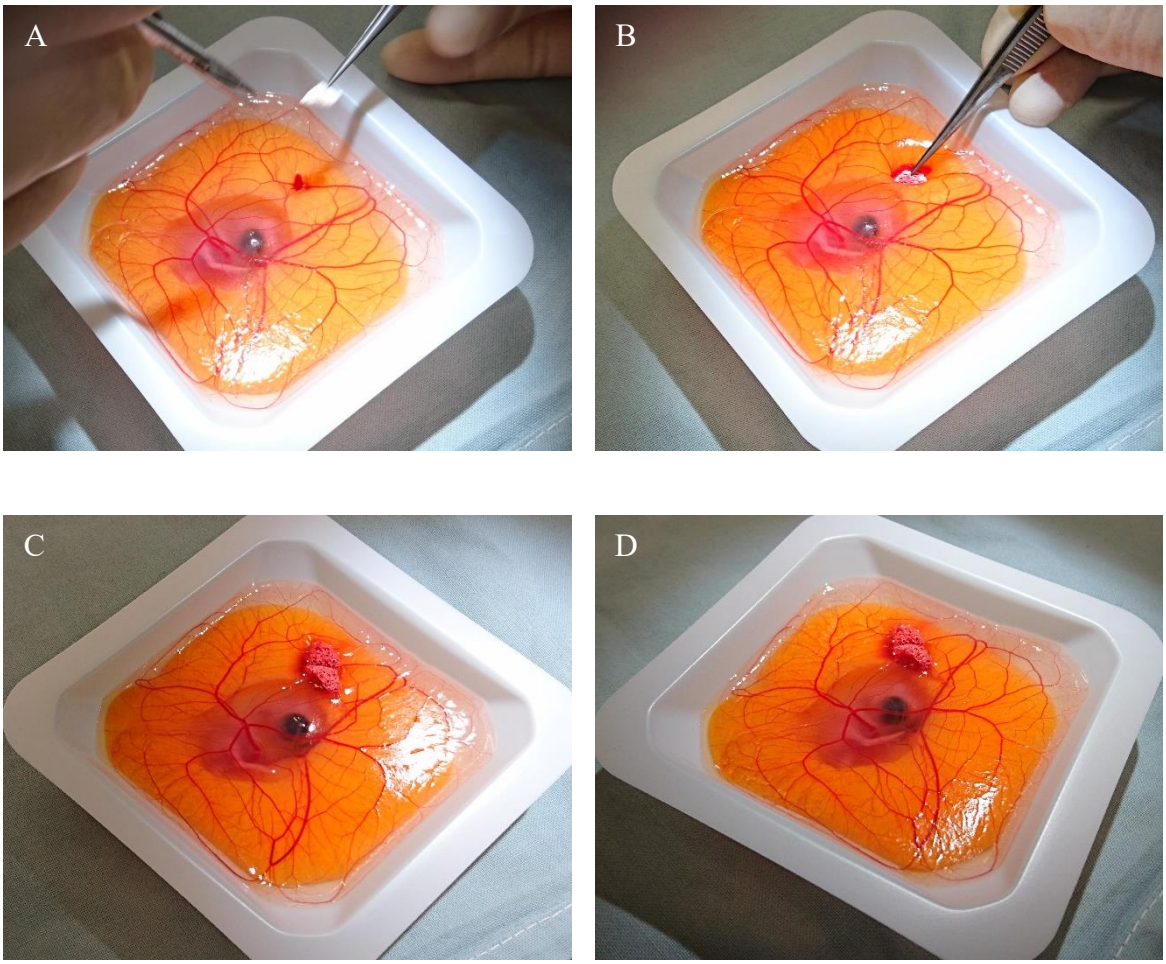

Figure 28: Blood stopping method

In the last two pictures of Figure 29, we want to show, that the removal of the sponge after about 5 min is possible and does not evoke a new bleeding.

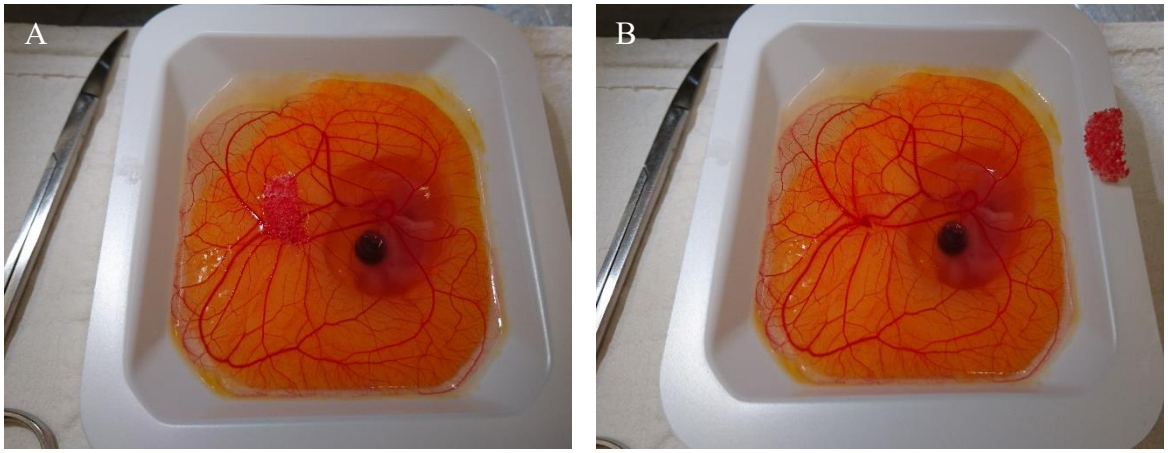

Figure 29: Removal of m-doc sponge

To find out if there are any differences in cutting venous or arterial vessels as well as to see how effective the m-doc sponges can stop bleeding and if the chicken embryos survive the whole process, we cut both – arterial and venous vessels – and made a follow up till day 14.

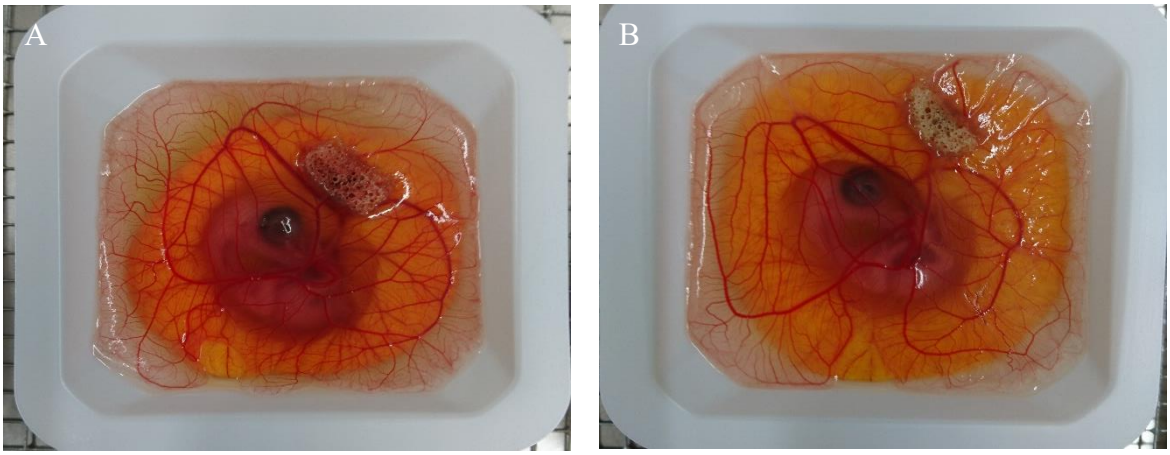

Figure 30: 3 days after blood stopping method

3 days after the whole process some of our treated chicken embryos were still alive, showing no differences to untreated ones. The little sponges could be removed 3 days after, too.

3 Results

3.1 Injection of Fluorescein 10%

Before starting our experiments with injecting Rose bengal, we tried to inject Fluorescein 10% and observed the distribution of the substance in the vascular system. We injected 0.26µl of the solution with a calculated dosage of 0.06µl/g. For the excitation we used an Olympus Stereo Microscope with an X-Cite 120 PC Fluorescence Light Source (120 W) and Fluorescence Filter Cubes.

These experiments were intended to show, that injections in the vascular system of a developing chicken embryo are possible.

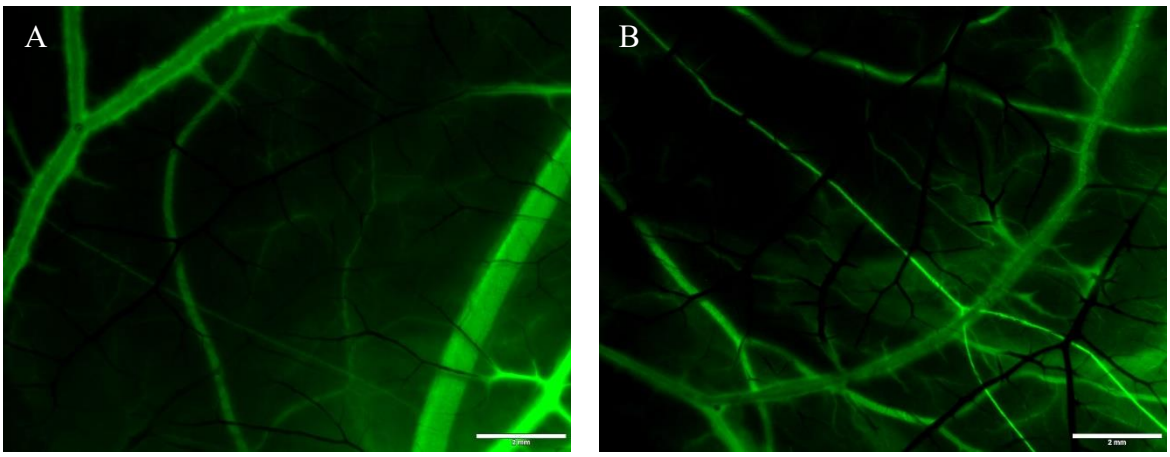

Figure 31: Green fluorescence of the CAM vessels

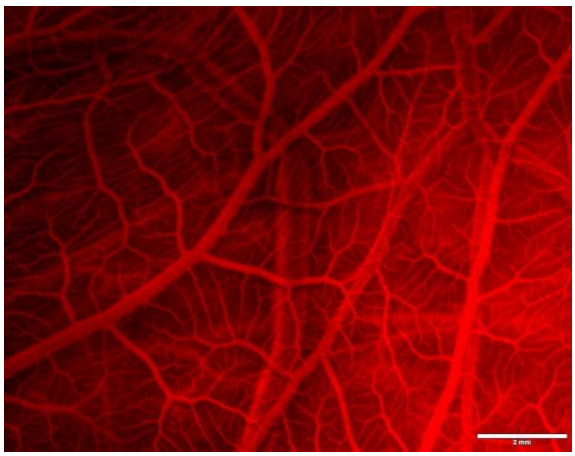

Figure 32: Vascular system without fluorescence

3.2 Protocol of Thrombus Formation

Rose bengal has been used in many experiments causing ischemic areas. Although it is not completely understood how Rose bengal induces thrombosis, it is most commonly associated with radical oxygen species (ROS) destroying the endothelial cells of the vessels. This process subsequently activates the clotting system.
To prove, that light activated Rose bengal causes thrombosis, a set of experiments was done.

Results:

1. Injection of PBS:

In the first series of experiments 3µl PBS were directly injected into the heart of a 5 days old embryo. The aim of this series was to show, that all changes in the vascular system of the developing embryo are induced by the activated Rose bengal, and not by any other substance or just by light irradiation with a wavelength of about 550nm.

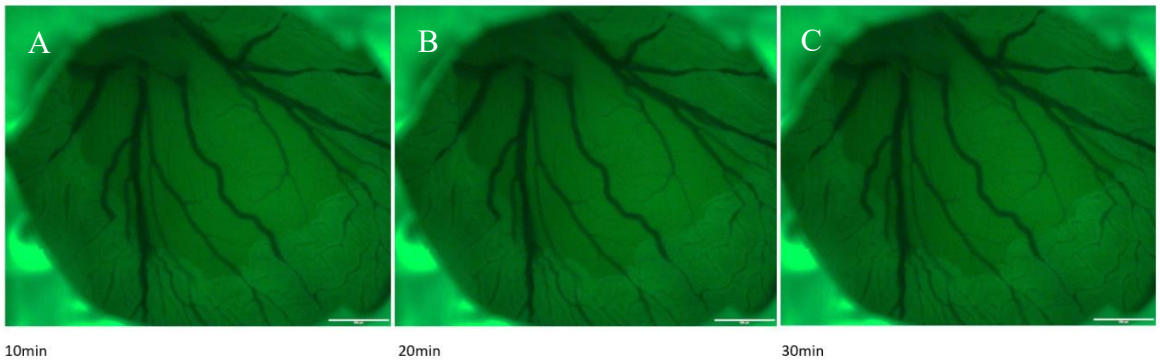

Figure 33: Heart injection of PBS

In Figure 33 A-C the illumination process can be followed step by step. The vascular system shows no differences before and after the light irradation for 30min using PBS. Neither any reduction of the lumen diameter, nor any other changes e.g. spasticity or shrinkage of the treated CAM area could be detected when injecting PBS.

2. Injection of Rose bengal with illumination:

In the second series we injected 3µl of a solution of Rose bengal of 50mg/ml concentration.

Figure 34: Heart injection of Rose bengal with illumination

Rose bengal right into the heart of the 5 days old embryo. Just as in series 1 we illuminated a selected area with green light for 30 minutes and took pictures every 10min.

Not only that the lumen of the vessels is smaller, but also a rarefaction of the whole vascular system can be observed. Since the chicken embryos died shortly after the treatment, further experiments need to differ between Rose bengal induced vessel changes and dying effects where peripheral capillaries in a dying embryo simply become more present before they start to disappear and dissolve from the periphery to the centre after the heartbeat has stopped.

In this series we assume an overlap of Rose bengal induced changes and beginning vessel changes because of the dying process.

3. Injection of Rose bengal without illumination:

The last series was intended to exclude vascular changes because of Rose bengal itself and not because of the activation of the substance by green light causing thrombosis.

Therefore 3µl of a solution of Rose bengal of 50mg/ml concentration was injected into the heart of a 5 days embryo without illumination with green light for 30min.

Figure 35: Heart injection of Rose bengal without illumination

The comparison before and after the treatment shows no significant changes, rarefaction or visible occlusions of any vessels. Little changes were attributed to the dying process.
To summarize, significant changes in the vascular system of the developing embryo can only be achieved by applying Rose bengal and illuminating it with green light for 30min.
Whether PBS, nor Rose bengal itself without activation, nor the dying process alone can cause such changes as seen in series 2. The chicken embryos of series 2 and 3 both died shortly after the pictures were taken, but only in series 2, where Rose bengal was illuminated for 30min, significant vessel changes could be observed.

3.3 Rose Bengal Photothrombosis in CAM

Figure 36 - 45 from chapter 3.3 and 3.4. show typical changes after an injection of 3µl of a 50mg/mL solution of Rose bengal in the vascular system of an 11 days old chicken embryo. In all the injection experiments the same concentration of Rose bengal was used and a typical pattern of vessel changes could be observed. During the first 4min of illumination with a green light lamp (525/50nm filter) the blood vessels seemed to show blood stasis and therefore minimal dilatation.

After 8min of illumination an obvious reduction of vessel density and a visible decrease of the vessel lumen could be seen. The whole area, that was illuminated also showed some shrinkage and the vessels appeared spastic.

After 10min of treatment the maximum effect seemed to be reached. No further noticeable changes could be observed afterwards.

All the documented figures shown in the diploma thesis originate from living chicken embryos, that survived the whole treatment:

- Laser Doppler Scanning before illumination
- Injection of 3µl of a 50mg/mL solution of Rose bengal
- Illumination process with green light laser (525/50nm filter) for 12 minutes
- Laser Doppler Scanning after illumination

Half of our treated chick embryos survived at least 9 hours, whilst the other half died about 2 hours after the process. Reasons for the death are discussed in detail in the discussion section and need further investigations in future experiments concerning the establishment of our wound healing model.

In a dying chick embryo a typical pattern of vessel changes can be detected. The lumen of vessels does not reduce or show spasticity as seen in rose bengal induced photothrombosis vessel changes. It seems as if peripheral capillaries in a dying embryo simply become more present before they start to disappear and dissolve from the periphery to the centre after the heartbeat has stopped.

3.3.1 Rose Bengal Photothrombosis in CAM without Human Split Skin Grafts

11 days old chicken embryo without human split skin, 3µL of a 50mg/mL Rose bengal injected.

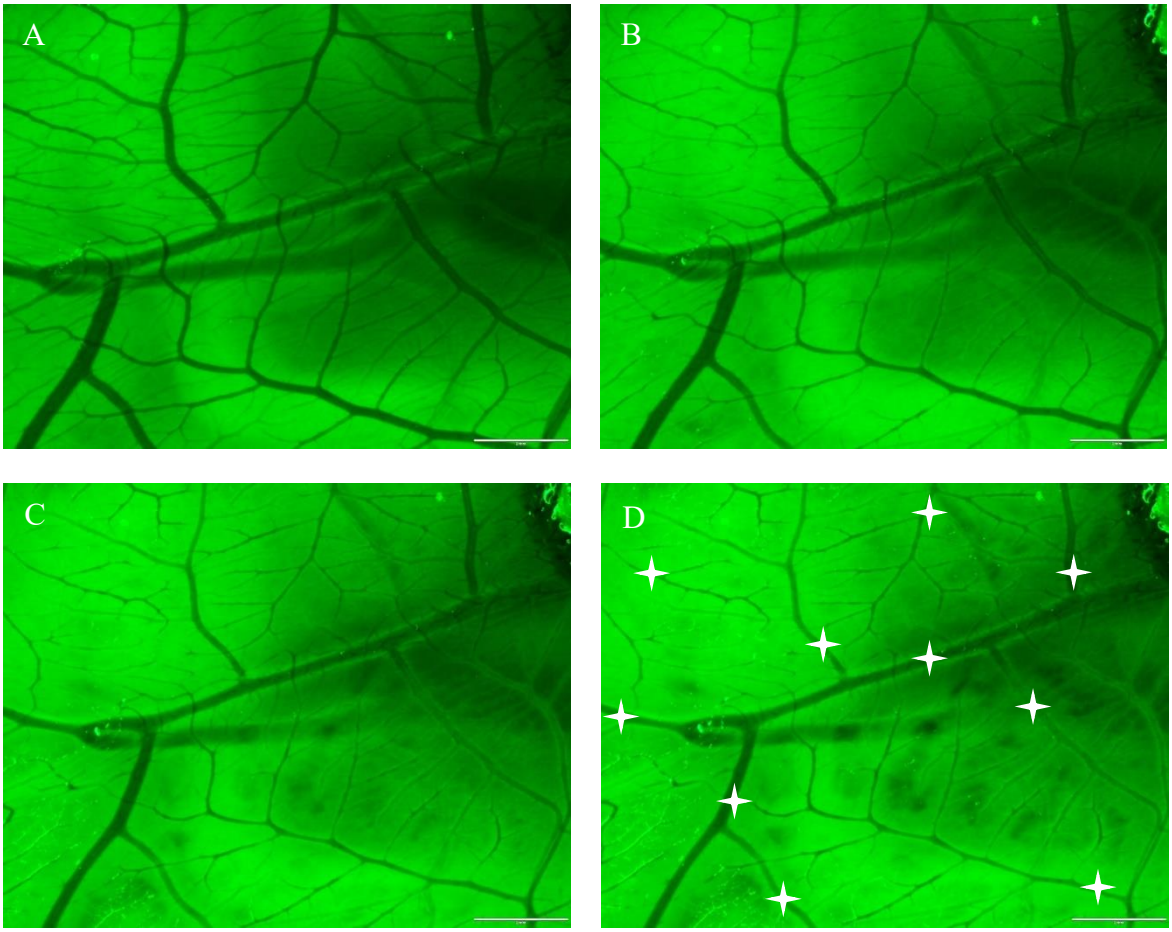

Figure 36: Rose bengal photothrombosis 1

A) before illumination (t0)
B) after 4min of illumination (t4)
C) after 8min of illumination (t8)
D) after 10min of illumination (t10)

In Figure 36 Rose bengal induced vessel changes can be followed step by step in CAM without split skin grafts. The pictures were taken during the illumination process with green-light. The reduction of the vessel diameters is the most obvious change observed in the whole illuminated area. In addition the spasticity of the vessels can be seen. Some vessels are marked with white spots to easily identify the changes.

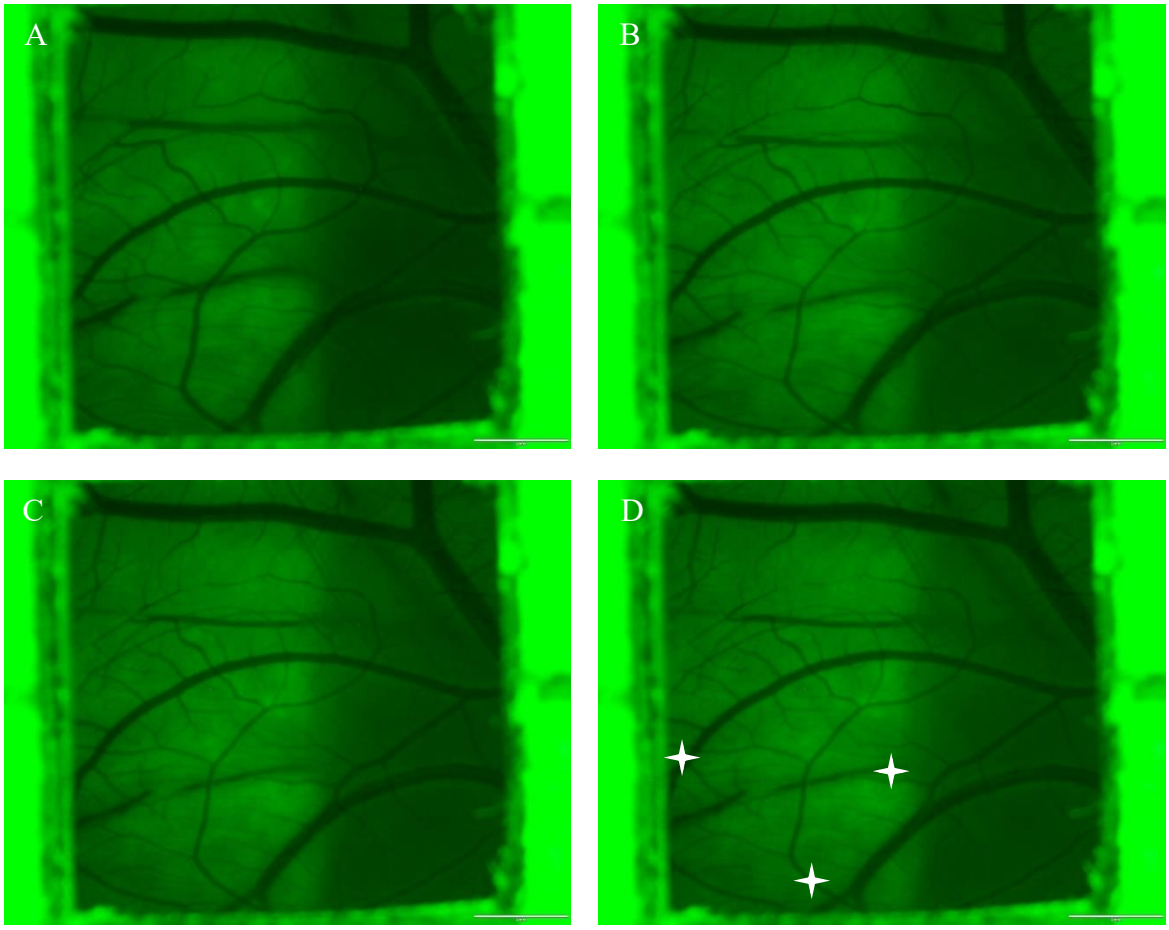

Figure 37: Rose bengal photothrombosis 2

A) before illumination (t0)
B) after 4min of illumination (t4)
C) after 8min of illumination (t8)
D) after 10min of illumination (t10)

Figure 37 also shows the step by step vessel changes induced by Rose bengal in CAM without split skin grafts. Since the vessel changes are not that obvious at first sight, some vessels with reduced lumen diameter are marked in Figure 37 D with white spots.

3.3.2 Rose Bengal Photothrombosis in CAM with Human Split Skin Grafts

11 days old chicken embryo with human split skin, 3µL of a 50mg/mL Rose bengal injected.

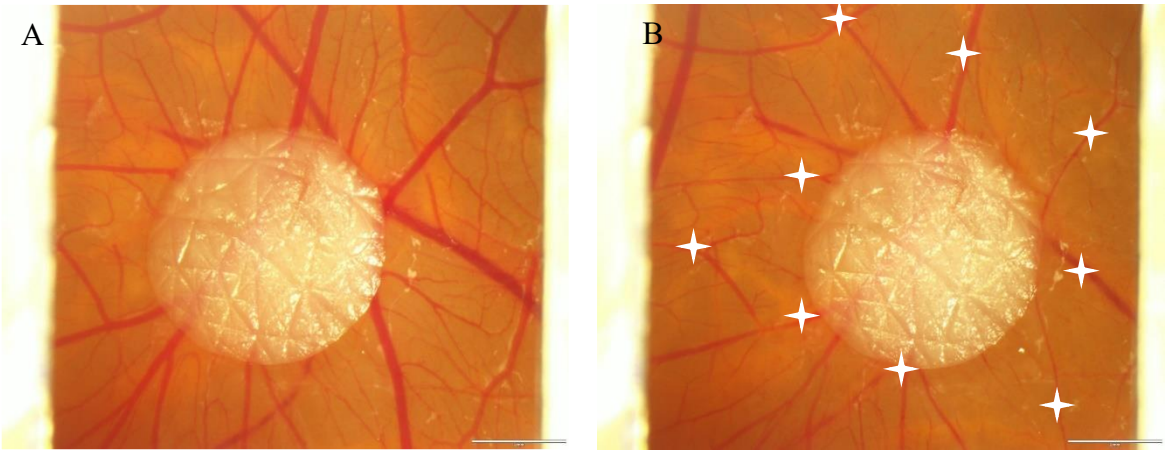

Figure 38: Rose bengal photothrombosis 3 - before and after 10 min illumination

In Figure 38 Rose bengal induced vessel changes in CAM with split skin grafts are shown before and after 10min of illumination. All the vessels around the split skin graft in the illuminated area - some were marked - show an obvious reduction of their lumen diameter.

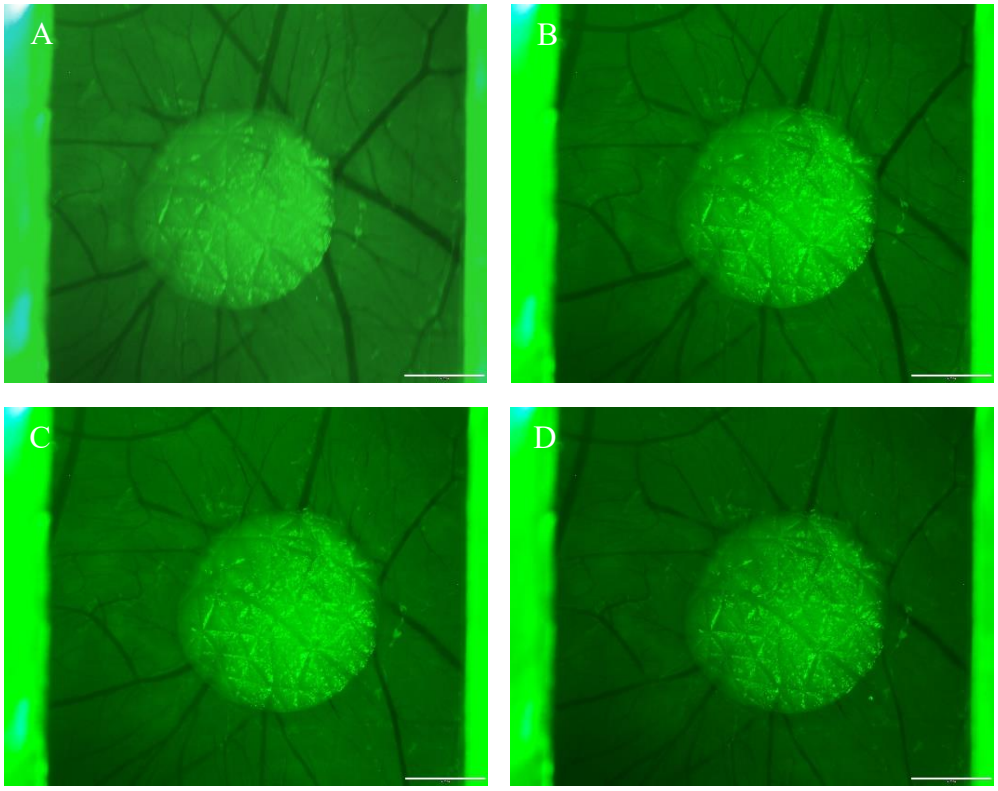

Figure 39: Rose bengal photothrombosis 3

A) before illumination (t0)

B) after 4min of illumination (t4)

C) after 8min of illumination (t8)

D) after 10min of illumination (t10)

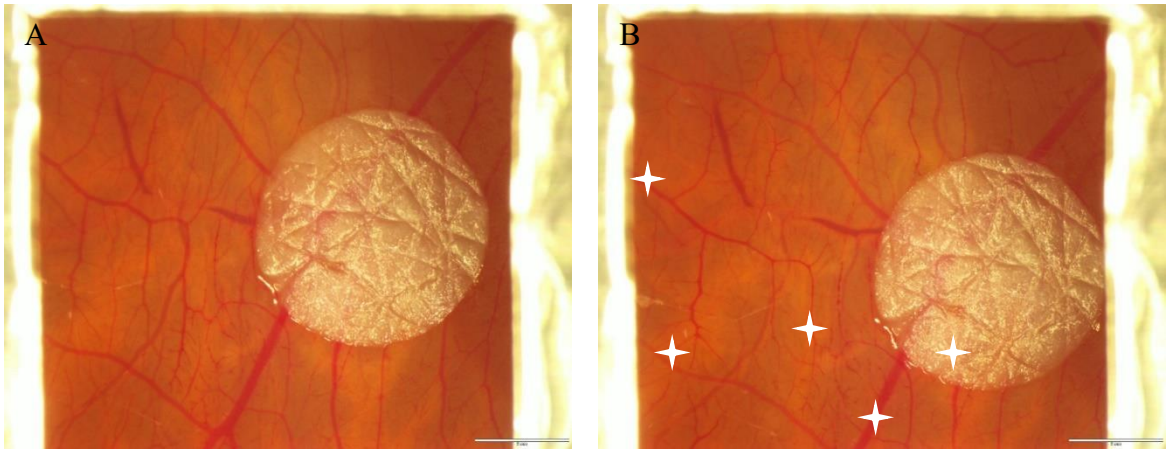

Figure 40: Rose bengal photothrombosis 4 - before and 10min after illumination

In Figure 40 Rose bengal induced vessel changes in CAM with split skin grafts are shown before and after 10min of illumination. Some of the vessels with lumen diameter reduction are therefore marked with white spots.

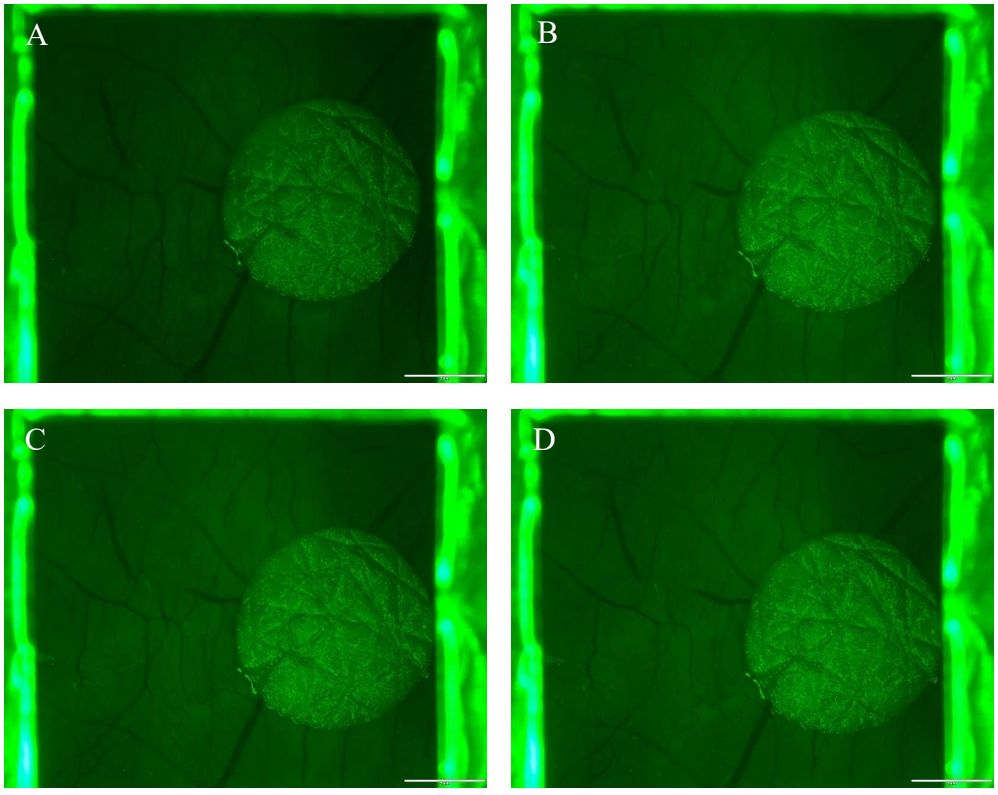

Figure 41: Rose bengal photothrombosis 4

A) before illumination (t0)

B) after 4min of illumination (t4)

C) after 8min of illumination (t8)

D) after 10min of illumination (t10)

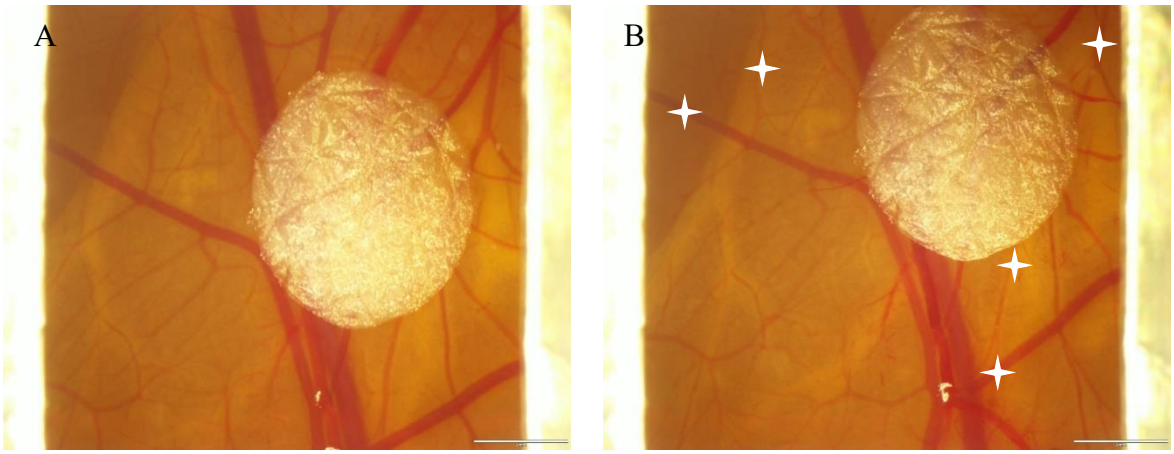

Figure 42: Rose bengal photothrombosis 5 - before and after 10min illumination

Figure 42 also shows Rose bengal induced vessel changes in CAM with split skin grafts before and after 10min of illumination. Although the changes are not always that obvious, the measurements show differences between before and after the treatment. Some of the vessels with lumen diameter reduction are marked with white spots.

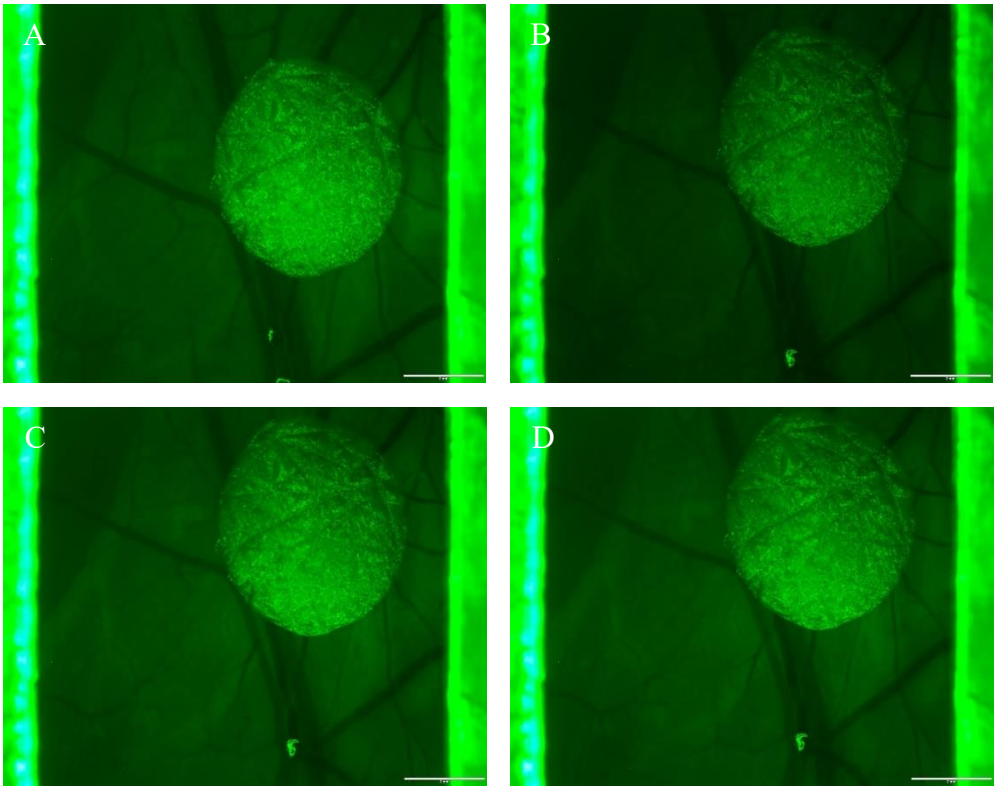

Figure 43: Rose bengal photothrombosis 5

A) before illumination (t0)

B) after 4min of illumination (t4)

C) after 8min of illumination (t8)

D) after 10min of illumination (t10)

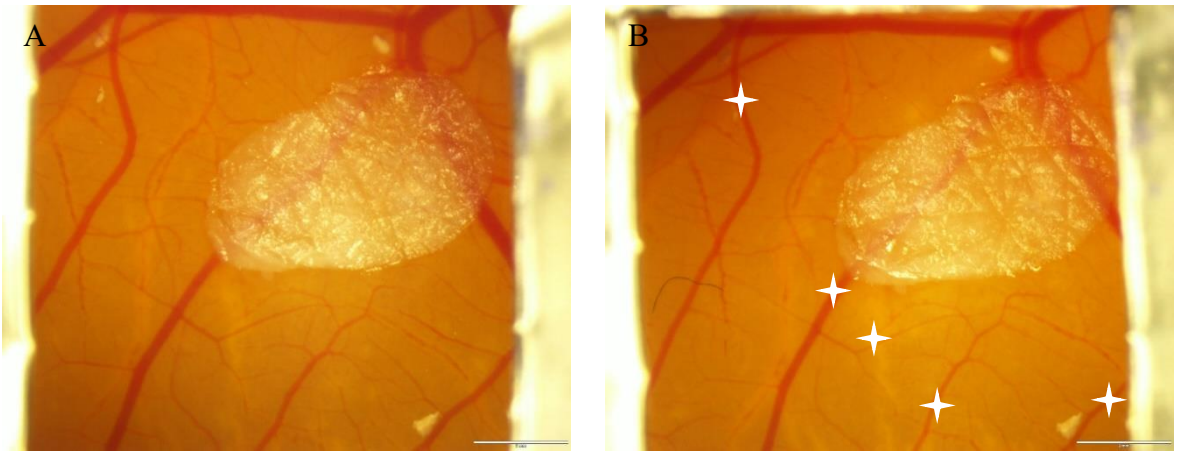

Figure 44: Rose bengal photothrombosis 6 - before and after 10min illumination

In Figure 44 Rose bengal induced vessel changes in CAM with split skin grafts are shown before and after 10min of illumination. Vessels with undergone lumen diameter reduction are marked with white spots.

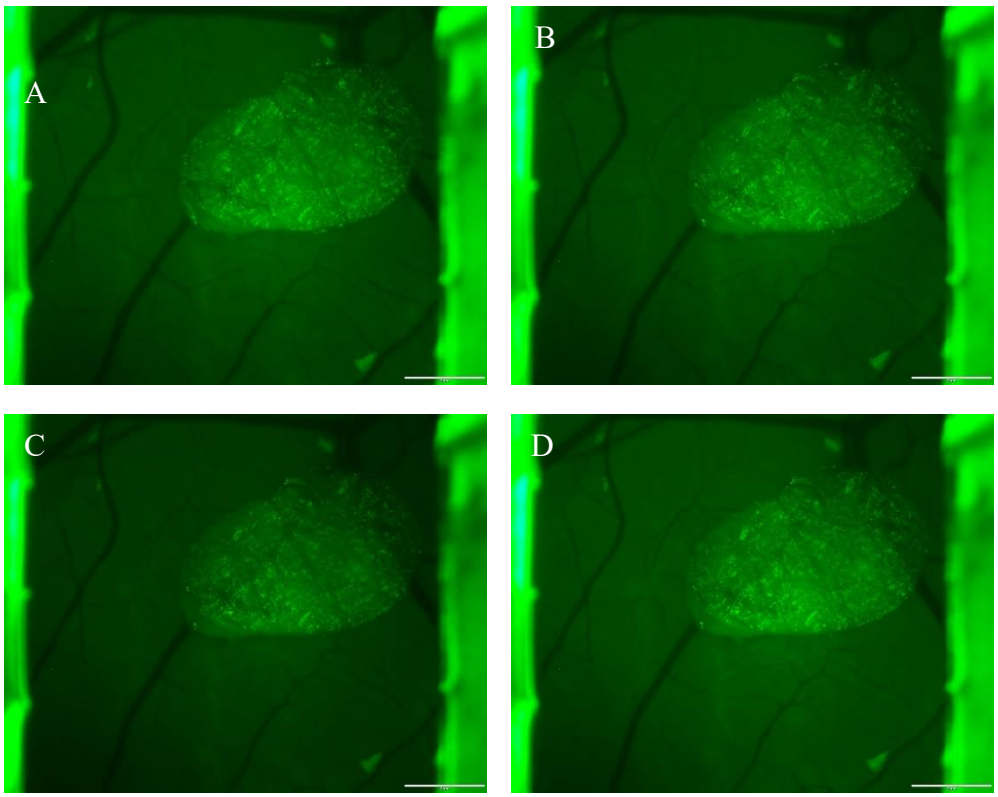

Figure 45: Rose bengal photothrombosis 6

A) before illumination (t0)

B) after 4min of illumination (t4)

C) after 8min of illumination (t8)

D) after 10min of illumination (t10)

3.4 Image Assessment of Rose Bengal induced Vessel Changes

To assess vessel changes in Rose bengal treated chick embryos we used the image program "cellSens Dimension 1.12" from Olympus Corporation.

We analysed the diameter of four representative blood vessels in our recorded pictures before as well as 10min after illumination and compared the changes.

Table 3: Vessel lumen assessment

Series (measured vessel)	Diameter in pixels (0min)	Diameter in pixels (10min)	Ratio before/after
Rose bengal photothrombosis 1 (1)	46.04	34.06	1/0.74
Rose bengal photothrombosis 1 (2)	37.01	19.42	1/0.52
Rose bengal photothrombosis 1 (3)	43.00	23.09	1/0.54
Rose bengal photothrombosis 1 (4)	64.08	52.08	1/0.81
Rose bengal photothrombosis 2 (1)	19.31	11.18	1/0.58
Rose bengal photothrombosis 2 (2)	34.53	22.20	1/0.64
Rose bengal photothrombosis 2 (3)	20.12	11.18	1/0.56
Rose bengal photothrombosis 2 (4)	41.87	36.24	1/0.87
Rose bengal photothrombosis 3 (1)	46.53	30.41	1/0.65
Rose bengal photothrombosis 3 (2)	42.20	12.08	1/0.29
Rose bengal photothrombosis 3 (3)	38.08	13.60	1/0.36
Rose bengal photothrombosis 3 (4)	30.41	18.44	1/0.61
Rose bengal photothrombosis 4 (1)	16.12	11.40	1/0.71
Rose bengal photothrombosis 4 (2)	14.56	7.00	1/0.48
Rose bengal photothrombosis 4 (3)	16.00	11.18	1/0.70
Rose bengal photothrombosis 4 (4)	14.14	10.20	0/0.72
Rose bengal photothrombosis 5 (1)	56.08	49.19	1/0.88
Rose bengal photothrombosis 5 (2)	37.12	23.35	1/0.63
Rose bengal photothrombosis 5 (3)	18.44	12.00	1/0.65
Rose bengal photothrombosis 5 (4)	37.66	27.17	1/0.72
Rose bengal photothrombosis 6 (1)	42.94	33.12	1/0.77
Rose bengal photothrombosis 6 (2)	18.36	13.93	1/0.76
Rose bengal photothrombosis 6 (3)	32.45	25.24	1/0.78
Rose bengal photothrombosis 6 (4)	36.40	24.84	1/0.68

Table 4: Overview vessel lumen assessment

Maximum of vessel lumen reduction	Minimum of vessel lumen reduction	Arithmetic Mean of vessel lumen reduction	Number of Vessels measured
71.37%	12.29%	34.84%	24

Table 5: Two-sample t-test for dependent samples (paired comparison test)

	Before treatment	*After treatment*
Mean	33.48	22.19
Variance	189.53	148.50
Observations	24	24
Pearson correlation	0.88	
Hypothetical difference of the mean	0	
Degrees of freedom (df)	23	
t-statistics	8.45	
p (T<=t) unilaterally	0.00000000827	
Critical t-value unilaterally	1.71	
p-value (bilaterally)	0.0000000165	
Critical t-value bilaterally	2.07	

To statistically assess the observed vessel changes a two-sample t-test for dependent samples (paired comparison test) was done using Excel 365 from Microsoft Office and SPSS.

The t-statistics (8.45) of the two-sample t-test for dependent samples (paired comparison test) is bigger than the critical t-value unilaterally. Thus the difference between before and after the treatment cannot be explained by the standard deviation. The p-value (T<=t) unilaterally is 0.00000000827. Since the α-Level was set by 0.05 the p-value is much smaller and therefore the decrease of the blood vessel diameter after the treatment with Rose bengal is statistically significant.

3.4.1 Assessment of Vascular Changes

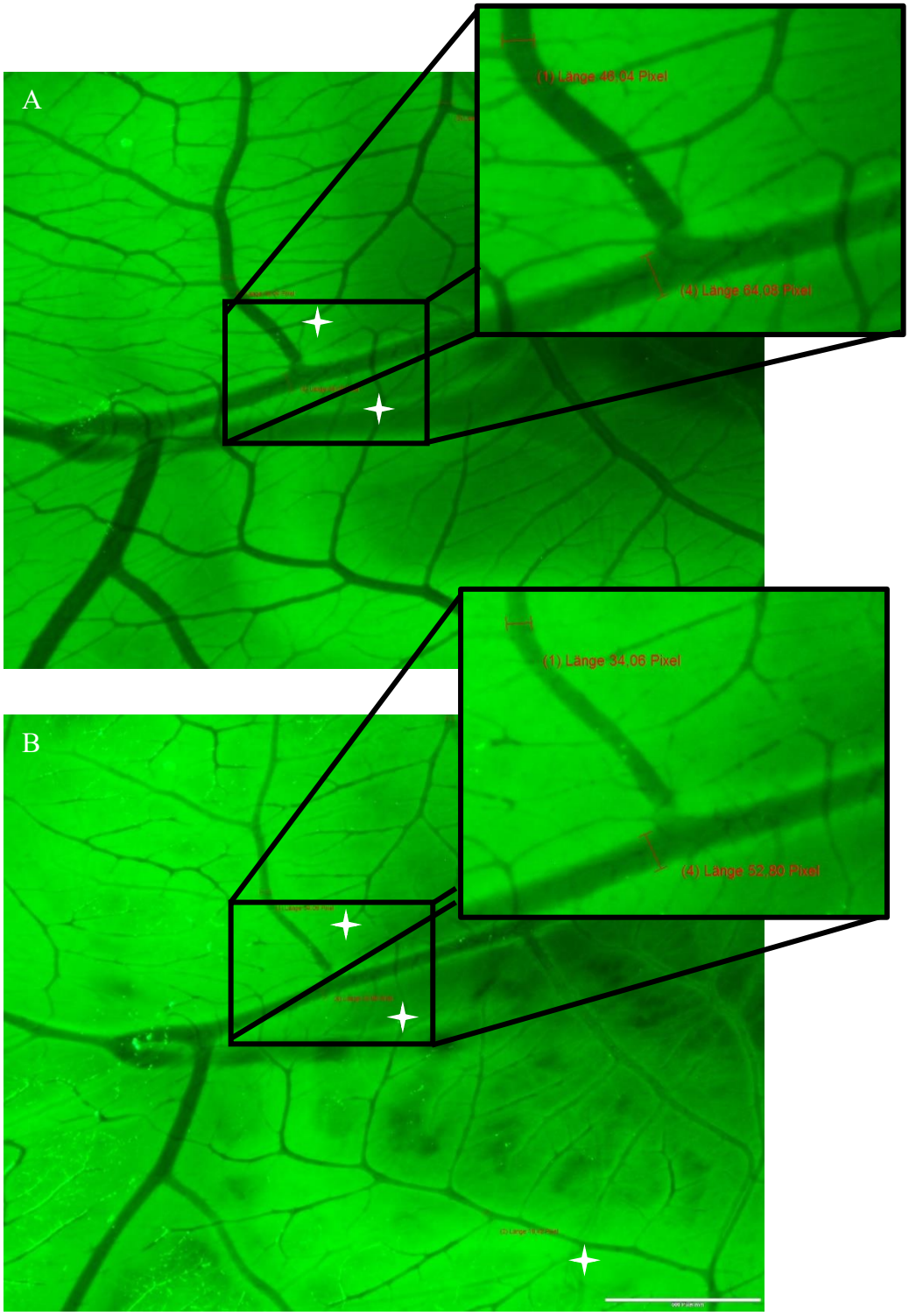

Figure 46: Example of vessel lumen assessment - before and after 10min illumination

Figure 46 shows an example of the lumen assessments done. In total 24 blood vessels (4 in each series) were measured before and after 10min illumination. Therefore a distance measurer was used. At right angles to the walls of the measured vessel the lumen diameter

could be detected in pixels and compared before and after the treatment. Afterwards the ratio before/after was calculated. The white spots mark the measured 4 vessels of “Rose bengal photothrombosis 1” shown in 3.3.1.

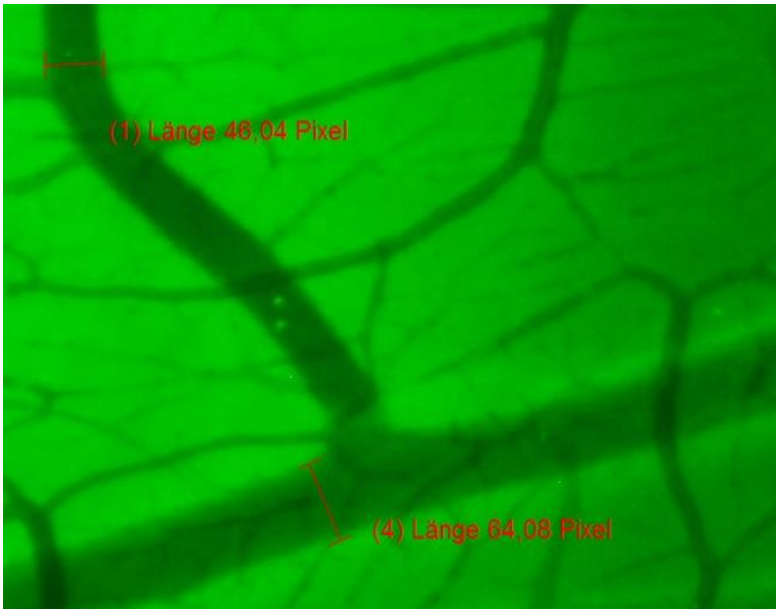

Figure 47: Lumen assessment

Figure 47 shows distance measurements set in 2 selected vessels in one of our series.

4 Discussion

As an intermediate stage between animal and human models the chick chorioallantoic membrane with xenografted human split skin seems to be the ideal model for testing new substances and therefore developing new therapies. Nowadays it is especially used for studying contact allergies in dermatology (37). Since the method of grafting human skin upon the CAM model has already been published in many papers, a successful implementation of it was possible. Criteria of viability for our skin grafts were easy to identify: after 3 days of incubation the skin showed a significantly thicker appearance based on cell proliferation (2) (37).

The major step for developing our wound healing model was the injection of Rose bengal in blood vessels of the chicken embryo. Since there exists no relevant paper treating this topic up to now, we had to establish the method. By the use of the ex-ovo method of chicken embryos (36), we could get better access to the blood vessels as well as the whole CAM. This enabled us to try injections into the veins, that are partially fixed in the CAM. For injections in these small vessels, special micro pipettes had to be pulled: thin enough to puncture the blood vessel, but thick enough to allow fluids to go macroscopically through. With the help of the Divison of Biophysics of the Medical University of Graz, this could be realised, too.

To prove that injections in CAM vessels can be achieved, we started with injections of fluorescein, before using Rose bengal. Injections are possible to be done but demand a long training time. The ideal time for CAM vessel injections was by day 10-11 of incubation, because then the vessels are big enough to be punctured and the chorioallantoic membrane is thin enough to get through.

Rose bengal is characterized in many papers, as photosensitive substance, that can easily be activated by the use of a laser or cold light lamp. When activated, it produces ROS, which destroy endothelial cells of the vessels and therefore induce the blood clotting cascade, forming thrombosis (42). Because of this phenomenon, we decided to use Rose bengal, since it enables the induction of local thrombosis, subsequently ischemia, without any effects on the rest of the organism. Only used in mouse and rat models for studying ischemic stroke, we were the first to use Rose bengal in CAM. Since there are important differences between mouse and rat models and the CAM, in particular a matured organism versus a developing one, we not only had to try different dosages, the induction of thrombosis, but also had to find out, if Rose bengal shows safety and tolerability in the developing chicken embryo. In "In vitro study for staining and toxicity of rose bengal on cultured bovine corneal endothelial

cells" by Lee Y.C. et. al., published 1996, they talk about an intrinsic toxicity of Rose bengal on endothelial cells, e.g. cell swelling, intracytoplasmic vacuole formation, cell detachment, and lysis, augmented by light illumination (49). Although, neither an actual toxicity testing is available, nor the authors of the papers in which mouse and rat models were used for Rose bengal induced stroke studies wrote about toxic effects.

In our model we injected 3µL (150µg) of a Rose bengal solution of 50mg/mL concentration. In relation to the concentrations used in mouse and rat models, we should have injected 250µg of Rose bengal in 10 days old chicken embryos. With considerations about a possible dosage dependent toxicity we used less. However, half of our treated chicken embryos survived 9 hours, the other half died about 2 hours after the injection process. This was the reason, why we assume a certain toxicity or intolerance of Rose bengal, maybe dosage dependent, in chicken embryos.

After the injection process, bleeding of the punctured vessel appeared. At this stage of chicken development, only a few millilitres of blood loss lead to death. By the means of testing different blood stopping substances, we finally chose little sponges with m-doc, an oxidised cellulose, that immediately stops superficial bleeding, without any influence on the organism. The sponges not only stop bleeding, but they absorb the blood and can afterwards, even a few days after, be easily removed. Since this method has not been used before, we cut CAM blood vessels of some chicken embryos with a scissor – to produce a huge bleeding – and treated the bleeding with the little sponges including m-doc. In about 2 seconds the bleeding stopped and with the sponge in place we put the chicken embryos back into the incubator to observe the survival. Interestingly many of the treated chicken embryos survived till day 14 of incubation without any problems.

The induction of photothrombosis was the next step. With references to "Photothrombotic ischemia: a minimally invasive and reproducible photochemical cortical lesion model for mouse stroke studies" by Vivien Labat-gest et. al. (50) we used a cold light lamp with a 525/50nm filter for activation of Rose bengal. The chosen CAM area was illuminated for 12min, although after 10min the maximum effect could be observed. In all the treated CAMs the same pattern of changes appeared: the diameter of the blood vessels got smaller, they appeared spastic and unregular, and the whole area seemed to be shrunk. To verify the visible reductions of blood vessels we measured the diameter of four representative ones before and 10min after the whole process with the program cellSens from Olympus. The data selected show that the 24 measured blood vessels in six different series undergo a reduction of their lumen on average of about 34.84%. The minimal observed reduction is

12.29% and the maximum is 71.37%. In contrast, some of the vessels seem to become bigger after the whole treatment. This may be because of blood stasis effects.

A two-sample t-test for dependent samples (paired comparison test) also showed, that the decrease of the blood vessel diameter after the treatment with Rose bengal is statistically significant (p-value 8.27E-09, α-value 0.05) and cannot be the effect of the standard deviation.

In summer 2018 we investigated pre-tests. These tests only showed vessel changes when used Rose bengal. Neither the injection of PBS with illumination, nor the injection of Rose bengal without illumination could produce any visible effects.

In conclusion, the grafting of human skin on the chick chorioallantoic membrane, the injection of Rose bengal in CAM blood vessels, the haemostasis of bleeding and the induction of photothrombosis are successfully implemented and described in the present diploma thesis. Only the follow-up of ischemic wounds was not yet possible, since the chicken embryos only survived hours after treatment, but not longer than one day.

Since all single steps of our experiments, e.g. grafting human skin on CAM, injection of PBS or fluorescein, haemostasis by m-doc and the illumination process without Rose bengal were tolerated by the chick embryos, we assume a certain dosage dependent toxicity of Rose bengal. Therefore a toxicity testing of Rose bengal in chicken embryos has to be done, before used in further experiments on the developing of our wound healing model. In addition to this, a dose finding study could be done. Another reason for death after the treatment could be the blood loss after the injection process. Even though quick haemostasis by m-doc sponges was possible, some millilitres of blood loss could not be prevented.

An important aspect for the success of our wound healing model is the follow-up of the Rose bengal treated and illuminated CAM area. Future studies have to show, whether the treated are becomes necrotic or induces neovascularisation. After proving neovascularisation a new series of experiments including human skin transplants can be undertaken to implement our wound healing model, to allow a follow-up till day 14 of incubation and furthermore to test the influence of substances on ischemic wounds.

Although there are many different models for wound healing in research, every model has its limitations. The only limitations of our wound healing model are the time window of 14 days, the lack of the immune system, the similarities to human beings and the lack of maturity of the organism. Since CAM experiments are only allowed for 14 days of embryological development – afterwards they are officially seen as animal testing - it is not possible to use our model for long-term studies. Another important aspect is the lack of the

immune system. Since the wound healing process consists of many different interacting cells, chemical substances and special environmental conditions our model can only be used to study the effect of therapies or new substances on single aspects of the wound healing process. It is not possible to study the complex interactions of the regeneration process when the immune system is not present. Furthermore it is known, that the best model for studying human skin regeneration at the moment seems to be the pig model, as it provides the majority of similarities. Nevertheless it is proved that even animal models do not reflect the wound healing process in the same way as it takes place in human species. With regards to our model, this means that observed phenomena can differ as well from humans. The last thing to keep in mind is that our model is based on an embryological developing organism. During embryological development biological processes often differ from those in mature organisms, e.g. because of different expressions of genes. Therefore other reactions of our model concerning testing substances or therapies may occur.

Finally, in-vitro and animal models can be useful for studying wound healing in basic research, but when it is about to develop new therapies for humans, we will not in the end be able to avoid human models to identify a significant influence of the new therapy or substance on the human wound healing process.

5 Bibliography

1. Heyer K, Herberger K, Protz K, Glaeske G, Augustin M. Epidemiology of chronic wounds in Germany: Analysis of statutory health insurance data. Wound Repair Regen Off Publ Wound Heal Soc Eur Tissue Repair Soc. 2016;24(2):434–42.

2. Kunzi-Rapp K, Rück A, Kaufmann R. Characterization of the chick chorioallantoic membrane model as a short-term in vivo system for human skin. Arch Dermatol Res. Mai 1999;291(5):290–5.

3. Wood FM. Skin regeneration: the complexities of translation into clinical practise. Int J Biochem Cell Biol. November 2014;56:133–40.

4. Lüllmann-Rauch R. Taschenlehrbuch Histologie. 4. Auflage. Stuttgart: Georg Thieme Verlag; 2012.

5. Agarwal S, Krishnamurthy K. Histology, Skin. In: StatPearls [Internet]. Treasure Island (FL): StatPearls Publishing; 2019 [zitiert 28. Mai 2019]. Verfügbar unter: http://www.ncbi.nlm.nih.gov/books/NBK537325/

6. Wong R, Geyer S, Weninger W, Guimberteau J-C, Wong JK. The dynamic anatomy and patterning of skin. Exp Dermatol. Februar 2016;25(2):92–8.

7. Hartmann M, Pabst MA, Dohr G. Zytologie, Histologie und Mikroskopische Anatomie - Licht- und elektronenmikroskopischer Bildatlas. 5. Auflage. Facultas; 2010.

8. Singer AJ, Clark RA. Cutaneous wound healing. N Engl J Med. 2. September 1999;341(10):738–46.

9. Schäffer M, Witte M, Becker H-D. Models to study ischemia in chronic wounds. Int J Low Extrem Wounds. Juni 2002;1(2):104–11.

10. Reinke JM, Sorg H. Wound repair and regeneration. Eur Surg Res Eur Chir Forsch Rech Chir Eur. 2012;49(1):35–43.

11. Krafts KP. Tissue repair: The hidden drama. Organogenesis. Dezember 2010;6(4):225–33.

12. Gurtner GC, Werner S, Barrandon Y, Longaker MT. Wound repair and regeneration. Nature. 15. Mai 2008;453(7193):314–21.

13. Rittié L. Cellular mechanisms of skin repair in humans and other mammals. J Cell Commun Signal. Juni 2016;10(2):103–20.

14. Sorg H, Tilkorn DJ, Hager S, Hauser J, Mirastschijski U. Skin Wound Healing: An Update on the Current Knowledge and Concepts. Eur Surg Res Eur Chir Forsch Rech Chir Eur. 2017;58(1–2):81–94.

15. Schreml S, Szeimies RM, Prantl L, Karrer S, Landthaler M, Babilas P. Oxygen in acute and chronic wound healing. Br J Dermatol. August 2010;163(2):257–68.

16. Martin P, Nunan R. Cellular and molecular mechanisms of repair in acute and chronic wound healing. Br J Dermatol. August 2015;173(2):370–8.

17. Morton LM, Phillips TJ. Wound healing and treating wounds: Differential diagnosis and evaluation of chronic wounds. J Am Acad Dermatol. April 2016;74(4):589–605; quiz 605–6.

18. Mustoe T. Understanding chronic wounds: a unifying hypothesis on their pathogenesis and implications for therapy. Am J Surg. Mai 2004;187(5A):65S-70S.

19. Tziotzios C, Profyris C, Sterling J. Cutaneous scarring: Pathophysiology, molecular mechanisms, and scar reduction therapeutics Part II. Strategies to reduce scar formation after dermatologic procedures. J Am Acad Dermatol. Januar 2012;66(1):13–24; quiz 25–6.

20. Metcalfe AD, Ferguson MWJ. Tissue engineering of replacement skin: the crossroads of biomaterials, wound healing, embryonic development, stem cells and regeneration. J R Soc Interface. 22. Juni 2007;4(14):413–37.

21. Profyris C, Tziotzios C, Do Vale I. Cutaneous scarring: Pathophysiology, molecular mechanisms, and scar reduction therapeutics Part I. The molecular basis of scar formation. J Am Acad Dermatol. Januar 2012;66(1):1–10; quiz 11–2.

22. Takeo M, Lee W, Ito M. Wound healing and skin regeneration. Cold Spring Harb Perspect Med. 5. Januar 2015;5(1):a023267.

23. Gottrup F, Agren MS, Karlsmark T. Models for use in wound healing research: a survey focusing on in vitro and in vivo adult soft tissue. Wound Repair Regen Off Publ Wound Heal Soc Eur Tissue Repair Soc. April 2000;8(2):83–96.

24. Wilhelm K-P, Wilhelm D, Bielfeldt S. Models of wound healing: an emphasis on clinical studies. Skin Res Technol Off J Int Soc Bioeng Skin ISBS Int Soc Digit Imaging Skin ISDIS Int Soc Skin Imaging ISSI. Februar 2017;23(1):3–12.

25. Ud-Din S, Bayat A. Non-animal models of wound healing in cutaneous repair: In silico, in vitro, ex vivo, and in vivo models of wounds and scars in human skin. Wound Repair Regen Off Publ Wound Heal Soc Eur Tissue Repair Soc. 2017;25(2):164–76.

26. Geris L, Schugart R, Van Oosterwyck H. In silico design of treatment strategies in wound healing and bone fracture healing. Philos Transact A Math Phys Eng Sci. 13. Juni 2010;368(1920):2683–706.

27. Seaton M, Hocking A, Gibran NS. Porcine models of cutaneous wound healing. ILAR J. 2015;56(1):127–38.

28. Moreno-Jiménez I, Hulsart-Billstrom G, Lanham SA, Janeczek AA, Kontouli N, Kanczler JM, u. a. The chorioallantoic membrane (CAM) assay for the study of human bone regeneration: a refinement animal model for tissue engineering. Sci Rep. 31 2016;6:32168.

29. Kue CS, Tan KY, Lam ML, Lee HB. Chick embryo chorioallantoic membrane (CAM): an alternative predictive model in acute toxicological studies for anti-cancer drugs. Exp Anim. 2015;64(2):129–38.

30. Cozigou G, Crozier J, Hendriksen C, Manou I, Ramirez-Hernandez T, Weissenhorn R. The European Partnership for Alternative Approaches to Animal Testing (EPAA): promoting alternative methods in Europe and beyond. J Am Assoc Lab Anim Sci JAALAS. März 2015;54(2):209–13.

31. Goodpasture EW, Douglas B, Anderson K. A STUDY OF HUMAN SKIN GRAFTED UPON THE CHORIO-ALLANTOIS OF CHICK EMBRYOS. J Exp Med. 31. Oktober 1938;68(6):891–904.

32. Dohle DS, Pasa SD, Gustmann S, Laub M, Wissler JH, Jennissen HP, u. a. Chick ex ovo culture and ex ovo CAM assay: how it really works. J Vis Exp JoVE. 30. November 2009;(33).

33. Ribatti D, Tamma R. The chick embryo chorioallantoic membrane as an in vivo experimental model to study human neuroblastoma. J Cell Physiol. Januar 2018;234(1):152–7.

34. Borges J, Tegtmeier FT, Padron NT, Mueller MC, Lang EM, Stark GB. Chorioallantoic membrane angiogenesis model for tissue engineering: a new twist on a classic model. Tissue Eng. Juni 2003;9(3):441–50.

35. Carre AL, Larson BJ, Knowles JA, Kawai K, Longaker MT, Lorenz HP. Fetal mouse skin heals scarlessly in a chick chorioallantoic membrane model system. Ann Plast Surg. Juli 2012;69(1):85–90.

36. Deryugina EI, Quigley JP. Chapter 2. Chick embryo chorioallantoic membrane models to quantify angiogenesis induced by inflammatory and tumor cells or purified effector molecules. Methods Enzymol. 2008;444:21–41.

37. Slodownik D, Grinberg I, Spira RM, Skornik Y, Goldstein RS. The human skin/chick chorioallantoic membrane model accurately predicts the potency of cosmetic allergens. Exp Dermatol. April 2009;18(4):409–13.

38. Andreassi A, Bilenchi R, Biagioli M, D'Aniello C. Classification and pathophysiology of skin grafts. Clin Dermatol. August 2005;23(4):332–7.

39. Kanapathy M, Smith OJ, Hachach-Haram N, Bystrzonowski N, Mosahebi A, Richards T. Systematic review and meta-analysis of the efficacy of epidermal grafting for wound healing. Int Wound J. Dezember 2017;14(6):921–8.

40. Herskovitz I, Hughes OB, Macquhae F, Rakosi A, Kirsner R. Epidermal skin grafting. Int Wound J. September 2016;13 Suppl 3:52–6.

41. Redmond RW, Kochevar IE. Review: Medical Applications of Rose Bengal- and Riboflavin-Photosensitized Protein Crosslinking. Photochem Photobiol. 20. Mai 2019;

42. Talley Watts L, Zheng W, Garling RJ, Frohlich VC, Lechleiter JD. Rose Bengal Photothrombosis by Confocal Optical Imaging In Vivo: A Model of Single Vessel Stroke. J Vis Exp JoVE. 23. Juni 2015;(100):e52794.

43. Kim J. The use of vital dyes in corneal disease. Curr Opin Ophthalmol. August 2000;11(4):241–7.

44. Watson BD, Dietrich WD, Busto R, Wachtel MS, Ginsberg MD. Induction of reproducible brain infarction by photochemically initiated thrombosis. Ann Neurol. Mai 1985;17(5):497–504.

45. Schroeter M, Jander S, Stoll G. Non-invasive induction of focal cerebral ischemia in mice by photothrombosis of cortical microvessels: characterization of inflammatory responses. J Neurosci Methods. 30. Mai 2002;117(1):43–9.

46. Maxwell KA, Dyck RH. Induction of reproducible focal ischemic lesions in neonatal mice by photothrombosis. Dev Neurosci. August 2005;27(2–4):121–6.

47. Piao MS, Lee J-K, Jang J-W, Kim S-H, Kim H-S. A mouse model of photochemically induced spinal cord injury. J Korean Neurosurg Soc. November 2009;46(5):479–83.

48. Pérez P, Alarcón M, Fuentes E, Palomo I. Thrombus formation induced by laser in a mouse model. Exp Ther Med. Juli 2014;8(1):64–8.

49. Lee YC, Park CK, Kim MS, Kim JH. In vitro study for staining and toxicity of rose bengal on cultured bovine corneal endothelial cells. Cornea. Juli 1996;15(4):376–85.

50. Labat-gest V, Tomasi S. Photothrombotic ischemia: a minimally invasive and reproducible photochemical cortical lesion model for mouse stroke studies. J Vis Exp JoVE. 9. Juni 2013;(76).

6 Appendix

6.1 Chemical Data Sheet: Rose Bengal

SIGMA-ALDRICH®

sigma-aldrich.com

3050 Spruce Street, Saint Louis, MO 63103, USA
Website: www.sigmaaldrich.com
Email USA: techserv@sial.com
Outside USA: eurtechserv@sial.com

Product Specification

Product Name:
Rose bengal - Dye content 95 %

Product Number:	**330000**
CAS Number:	632-69-9
MDL:	MFCD00151169
Formula:	C20H2Cl4I4Na2O5
Formula Weight:	1,017.64 g/mol

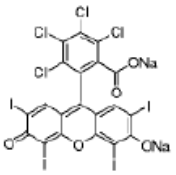

TEST	Specification
Appearance (Color)	Red to Brown
Appearance (Form)	Conforms
Powder and/or Chunks	
Infrared spectrum	Conforms to Structure
Wave Length	546 - 550 nm
c = 0.004g/L H2O + 1ml 1% Na2CO3	
Extinction Coefficient	≥ 98000
Wave Length	513 - 517 nm
Extinction Coefficient	≥ 32000
Wave Length	350 - 354 nm
Extinction Coefficient	≥ 3000
Wave Length	311 - 315 nm
Extinction Coefficient	≥ 12000
Wave Length	262 - 266 nm
Extinction Coefficient	≥ 32000
Purity (HPLC)	≥ 95.0 %
Approximately	

Specification: PRD.0.ZQ5.10000024860

Synonym: 4,5,6,7-Tetrachloro-2′,4′,5′,7′-tetraiodofluorescein disodium salt, Acid Red 94, Bengal Rose B sodium salt, Rose bengal sodium salt

PubChem Substance ID: 24859827

Absorption: λ_{max} 549nm